Balanced Dynamics and Convection in the Tropical Troposphere

David J. Raymond*, Željka Fuchs, Saška Gjorgjievska, and Sharon L. Sessions
Physics Department and Geophysical Research Center
New Mexico Tech
Socorro, NM, USA

June 8, 2015

Key points:

- Balanced dynamics and convection work together in the tropics.
- Observations of convection provide insight into balanced tropical flows.

*Corresponding author: raymond@kestrel.nmt.edu.

Abstract

This paper presents a conceptual picture of balanced tropical tropospheric dynamics inspired by recent observations. The most important factor differentiating the tropics from middle and higher latitudes is the absence of baroclinic instability; upward motion occurs primarily via deep convective processes. Thus, convection forms an integral part of large-scale tropical motions. Since convection itself is small-scale and chaotic in detail, predictability lies in uncovering the hidden hands that guide the average behavior of convection. Two appear, balanced dynamics and thermodynamic constraints. Contrary to conventional expectations, balanced dynamics plays a crucial role in the tropical atmosphere. However, due to the smallness of the Coriolis parameter there, non-linear balance is more important in the tropics than at higher latitudes. Three thermodynamic constraints appear to play an important role in governing the average behavior of convection outside of the cores of tropical storms. First, convection is subject to control via a lower tropospheric buoyancy quasi-equilibrium process, wherein destabilization of the lower troposphere by non-convective processes is balanced by convective stabilization. Second, the production of precipitation is extraordinarily sensitive to the saturation fraction of the troposphere. Third, "moisture quasi-equilibrium" governs the saturation fraction, with moister atmospheres being associated with smaller moist convective instability. The moist convective instability is governed by the balanced thermodynamic response to the pattern of potential vorticity, which in turn is slowly modified by convective and radiative heating. The intricate dance between these dynamic and thermodynamic processes leads to complex behavior of the tropical atmosphere in ways that we are just beginning to understand.

Index terms and keywords: 3303 Balanced dynamical models; 3314 Convective processes; 3354 Precipitation; 3371 Tropical convection; 3373 Tropical dynamics.

1 Introduction

In middle latitudes, quasi-geostrophic dynamics provides a zeroth order picture of how the atmospheric circulation works. Due to the small values of the Coriolis parameter in the tropics, the role of balanced dynamics there is generally deprecated. However, a careful analysis of tropical dynamics suggests that this point of view may be over-emphasized. The *Wheeler and Kiladis* [1999] analysis of tropical wave modes isolates a number of fast-moving disturbances in which gravity wave dynamics are clearly important, such as the equatorial Kelvin wave, eastward-moving mixed Rossby-gravity waves, and inertia-gravity waves. However, equatorial Rossby waves, easterly waves, monsoon lows, tropical cyclones, the Madden-Julian oscillation, and the Hadley circulation all exhibit strong potential vorticity signatures, indicating a significant role for balanced dynamics in their formation and evolution.

The biggest difference between balanced dynamics in the tropics and middle latitudes is that horizontal temperature gradients are much weaker in the tropics. Since most balanced vertical motion occurs via isentropic upglides that require strong horizontal temperature gradients to operate, balanced dry ascent is weak in tropical regions. Most vertical motion there is provided by a combination of deep moist convection and radiative cooling. Thus, convective and radiative processes which are important but not dominant in middle latitude dynamics, play crucial roles in the tropics. Any zeroth order theory of tropical dynamics must account for the interplay of convection, radiation, and balanced dynamics.

In this paper we first consider two seminal contributions to the dynamics of the tropics, *Ooyama's* [1982] paper on tropical cyclones, and the work of *Sobel and Bretherton* [2000] and *Sobel et al.* [2001] on the weak temperature gradient approximation. Ooyama points out that only the balanced part of tropical flows is likely to be predictable. Furthermore, balanced dynamics takes a particularly simple form in the weak temperature gradient case.

We then turn our attention to tropical convection, considering especially the manner in which convection is forced. *Ooyama* [1982] highlights the importance of relating convection to the balanced part of the flow, as the unbalanced part is tightly coupled to the convection itself. The time required to establish balance is often shorter than the time scale over which convection modifies the vorticity pattern, thus providing the scale separation necessary to make possible the parameterization of convection. In this picture, only the average behavior of convection over balanced dynamics time scales is parameterizable; convective fluctuations on smaller time scales are considered to be unpredictable and chaotic.

Ooyama [1982] views tropical cyclones as systems in which the rotational time scale (i.e., the time required to establish balance) decreases to values comparable to the time scale of convective overturning, though he expressed this relationship in terms spatial scales and the Rossby radius. In this "cooperative intensification" picture, the convection is tightly controlled by frictional convergence, thus minimizing the tendency for chaotic behavior. Ooyama is quick to point out that this mechanism fails in less extreme situations due to the longer time scales of balanced flows. Any attempt to extend the cooperative intensification process of cyclones to the tropics in general is therefore ill-conceived. However, potential vorticity dynamics still provides a framework for understanding the effects of convection on the balanced flow, e.g., *Hoskins et al.* [1985], *Haynes and McIntyre* [1987, 1990], *Raymond*

[1992] and thermodynamic mechanisms can act to control the average behavior of convection.

The powerful idea of quasi-equilibrium between convection and the large-scale, which is assumed to exhibit time scales much longer than those of convection, was introduced by *Arakawa and Schubert* [1974] and developed further by *Emanuel et al.* [1994]. Various iterations of this concept have converged to the idea that convection responds rapidly to changes in the lower tropospheric parcel buoyancy, which in turn is controlled by the virtual temperature profile in the lower troposphere and the boundary layer moist entropy. Though many have contributed to this development, *Kuang* [2008a,b] has perhaps demonstrated lower tropospheric quasi-equilibrium most convincingly.

Needed in addition is a knowledge of the effects of changes in the tropical convective environment on the form of convection. Observational and related numerical work on the dynamics of tropical cyclone precursor disturbances [*Raymond et al.,* 2011; *Gjorgjievska and Raymond*, 2014; *Raymond et al.*, 2014] have led to surprising results in this regard. Larger values of column relative humidity as well as stronger latent and sensible surface heat fluxes lead to more rainfall. The cloud-resolving modeling results of *Derbyshire* [2004], *Raymond and Sessions* [2007], *Kuang* [2008a], and *Sessions et al.* [2015] support this picture.

However, a decrease in moist convective instability in the form of a cooler environment in the lower troposphere and/or a warmer environment in the upper troposphere also leads to enhanced rainfall, e.g., *Raymond and Sessions* [2007], *Raymond et al.* [2011], *Gjorgjievska and Raymond* [2014], *Raymond et al.* [2014], and *Sessions et al.* [2015]. In addition, such a temperature dipole causes the vertical mass flux profile to be more bottom-heavy, with profound implications for the formation of tropical cyclones. These temperature anomalies appear largely to be a balanced response to the vorticity pattern in the atmosphere, forming yet another link between convection and balanced dynamics [*Raymond*, 2012].

Another interesting result of this and other research [*e.g.*, *Ramage*, 1971; *Williams et al.*, 1992; *Singh and O'Gorman*, 2013] is that there appears to be a negative correlation between humidity and moist convective instability; the more stable the environment, the higher the humidity. According to *Singh and O'Gorman* [2013], this correlation is due to the response of the convection itself to variations in convective instability; an environment that is too dry for the existing profile of convective instability results in convection that loses buoyancy from entrainment, thus detraining moist air into the environment. An overly moist environment produces vigorous convection that dries the atmosphere. This feedback process, which we name "moisture quasi-equilibrium", drives the environment toward a critical value of tropospheric relative humidity.

The column-integrated moist entropy (or moist static energy) budget turns out to be a crucial factor in moist convection [*Back and Bretherton*, 2006; *Raymond et al.*, 2009]. If horizontal temperature gradients are weak, then the entropy budget turns out to be essentially a budget for column-integrated water vapor. The entropy budget has the advantage over the water vapor budget in that the water vapor tendency in the latter is the result of a small residual between moisture convergence and precipitation and is therefore almost impossible to compute in observations. Due to the conservation properties of the moist entropy, the precipitation does not enter into the moist entropy budget. If moist entropy is exported in large quantities from the convective region, then the region dries out and the propensity

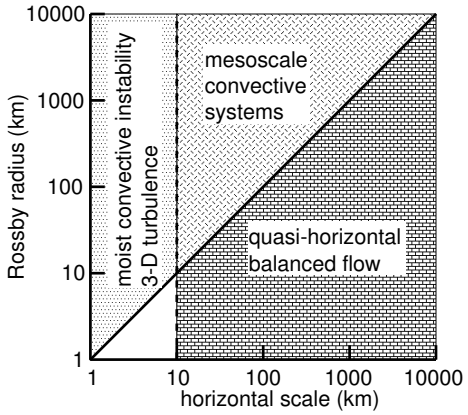

Figure 1: After figure 1 in *Ooyama* [1982].

for future convection is decreased. On the other hand, if the positive contribution to the entropy budget of surface fluxes exceeds the negative contributions of radiation and lateral export, then the propensity for future convection is increased due to the net moistening of the column. Thus, the future evolution of convection is controlled to a large degree by the entropy budget.

Section 2 discusses the ideas of *Ooyama* [1982]. The weak temperature approximation is considered in section 3. Potential vorticity dynamics are reviewed in section 4 and the interaction of convection with the balanced flow is discussed in section 5. Discussion and conclusions are presented in section 6.

2 Ooyama and tropical cyclones

An excellent starting point for any discussion of tropical atmospheric dynamics is the paper by *Ooyama* [1982]. Though this paper is focused on the theory of tropical cyclones, it contains important lessons for the subject as a whole. Ooyama emphasizes that a clean separation between moist convection and the large-scale flow exists only when "large scale" is defined as that part of the flow nearly in balance. This is because convective circulations consist of much more than the highly localized non-hydrostatic flow associated with the visible convective cloud. The invisible return circulation for the visible convection extends out to the Rossby radius of deformation in a complicated, time-dependent manner [*see Bretherton and Smolarkiewicz,* 1989]. Furthermore, it is so closely coupled with the visible circulation that it has no independent existence, disappearing shortly after the visible convection dissipates. This return circulation is therefore scarcely less complex than the convection to which it is coupled. In contrast, the balanced part of the flow, though it can be modified by the convection, exists before the convection develops and continues to exist after the convection is gone. Furthermore, the balanced circulation responds primarily to the space- and time-integrated properties of the convection and is thus insensitive to small-scale, transient details.

Figure 1, which is an adaptation of *Ooyama's* [1982] figure 1, illustrates this point. The horizontal axis represents the horizontal scale of a disturbance while the vertical axis represents the Rossby radius. The diagonal line divides the domain into disturbances with horizontal scale larger than the Rossby radius, representing nearly horizontal balanced flow, and disturbances with horizontal scale smaller than the Rossby radius. The latter are subdivided into hydrostatic and non-hydrostatic disturbances separated by the dashed vertical line. Ooyama puts the flows associated with the visible convective cloud as well as three-dimensional turbulence in the non-hydrostatic category while characterizing the hydrostatic region as the domain of "mesoscale convective systems". This is clearly a dynamical rather than a scale-based definition, as it includes tropical disturbances of rather large spatial scales such as convectively coupled equatorial Kelvin waves.

Dynamically, the difference between balanced and unbalanced flow is more succinctly represented by a time scale T rather than a spatial scale. On an f-plane with relative vorticity small in magnitude compared to the Coriolis parameter f, a Rossby number

$$\mathrm{Ro} = \frac{1}{Tf} \tag{1}$$

of unity divides the two domains, with $\mathrm{Ro} \ll 1$ representing balanced flow and $\mathrm{Ro} \gg 1$ representing unbalanced flow. On the equator where $f = 0$, there technically is no balanced regime since $\mathrm{Ro} = \infty$ there. However, this analysis must be modified if there is significant absolute vorticity ζ near or even on the equator. In this case we can generalize the definition of Rossby number by replacing f with ζ:

$$\mathrm{Ro} = \frac{1}{T\zeta}. \tag{2}$$

Taking $\mathrm{Ro} = 1$ as the critical value separating balanced and unbalanced flow yields a critical time scale

$$T_B = \frac{1}{\zeta}. \tag{3}$$

Disturbances with time scales much longer than T_B are nearly balanced while much shorter time scales indicate unbalanced flow. For weak disturbances near 15° latitude with $\zeta \approx f$, the critical time scale is $T_B \approx 7\,\mathrm{hr}$. In the case of a developing tropical cyclone at the same latitude, we can easily have $\zeta \approx 10f$, which yields $T_B \approx 45\,\mathrm{min}$. Strong tropical cyclones exhibit much smaller values of T_B than this in their central regions.

The relationship between Rossby radius and this balance time scale depends on one additional variable, the depth of the disturbance in question, or more precisely, the speed of hydrostatic gravity waves with this vertical scale. If h is half the vertical wavelength of a gravity wave, the horizontal speed of the wave is

$$c = \frac{hN}{\pi} \tag{4}$$

where N is the Brunt-Väisälä frequency of the atmosphere. The Rossby radius is conventionally defined

$$\lambda = cT_B = \frac{hNT_B}{\pi}. \tag{5}$$

Assuming a weak disturbance near 15° latitude, $h = 15\,\mathrm{km}$ (fundamental baroclinic mode), and $N = 10^{-2}\,\mathrm{s}^{-1}$, we have a Rossby radius of $\lambda \approx 1200\,\mathrm{km}$, whereas for a mid-level vortex in a developing tropical storm with a vertical scale of 5 km and $\zeta = 10f$, we have $\lambda \approx 40\,\mathrm{km}$. Thus, the Rossby radius can vary over a wide range for different conditions in the tropics, making the term "large scale" for the balanced regime somewhat of a misnomer. The critical time is a much less volatile quantity than the Rossby radius.

Ooyama's central argument is that to the extent that tropical convection is subject to external control beyond thermodynamic factors, this control is likely to come from the balanced component of the flow, as this is the only aspect of the tropical circulation with an existence independent of the convection itself. The essential nature of this control has been extremely difficult to sort out. *Ooyama's* [1964, 1969, 1982] ideas on the subject apply specifically to the inner core of an intensifying tropical cyclone. In this case, the Rossby radius is small enough that a particular form of the balanced control of convection, frictional convergence, is applicable; frictionally induced boundary layer convergence drives deep convection that promotes the spinup of the cyclone vortex through a deep layer. Convective entrainment in this layer draws in air from the surroundings, resulting in spinup in the free troposphere via the conservation of absolute angular momentum. The balanced response to the intensifying deep vortex is a lowering of the surface pressure and consequent strengthening of the surface vortex.

Ooyama prefers to call this "cooperative intensification", but accedes reluctantly to the term "CISK" for Convective Instability of the Second Kind, which was invented by *Charney and Eliassen* [1964], to describe this process. This latter paper has been subject to a great deal of justifiable criticism due to the fact that it is incomplete in several respects; in particular it ignores the crucial role of surface heat fluxes in the energetics of tropical cyclones and it linearizes the highly nonlinear cooperative intensification process [*Ooyama,* 1982; *Emanuel*, 1986].

Ooyama [1982] also objects to the indiscriminate application of the cooperative intensification mechanism to situations in which the underlying assumptions are not justified. In particular, if the Rossby radius in the disturbance of interest is larger than the disturbance itself, then the flow in the disturbance is fundamentally unbalanced, and the unbalanced winds associated with the convection itself typically dominate the balanced frictional convergence. In this case the convection is subject primarily to thermodynamic control. This is likely to be true in the early stages of tropical cyclone formation, in easterly waves and other similar systems, and in variability along the intertropical convergence zone [ITCZ; *see Raymond et al.*, 2006].

The bottom line is that the cooperative intensification mechanism of Ooyama is alive today, but it is a special case that applies mainly in the highly rotational environment of a tropical cyclone; attempts to apply it to other situations are generally ill-considered. The work of *Emanuel* [1986] and *Rotunno and Emanuel* [1987], though critical of *Charney and Eliassen* [1964], is really an extension of Ooyama's idea that considers the ascending and outflow branches of the tropical cyclone to be balanced, neutrally buoyant, and non-entraining.

Smith and Montgomery [2008] and *Montgomery and Smith* [2014] show that the boundary layer flow in a tropical cyclone is not balanced in the traditional sense, in that the radial advection of angular momentum remains important there. However, this flow is still slaved

to the overlying pressure distribution, which is a consequence of balanced processes in the free troposphere.

An obvious question is whether the class of balanced disturbances in the tropics includes anything but tropical cyclones. This boils down to whether the divergence time scale (just the inverse of the divergence) is greater than or less than the time required to establish balanced flow, T_B. In the former case balance is established rapidly compared to the time scale over which the vorticity evolves under the influence of divergence (primarily convection-related); in the latter case the vorticity evolves faster than balance can be established, and the flow is essentially unbalanced. In the time window between T_B and the divergence time scale, the vorticity is in control of the convection rather than vice versa.

Certain disturbances such as easterly waves retain vorticity signatures for many days, which is well in excess of plausible values of T_B. Thus, such disturbances can be classed as balanced. The recent work of *Yasunaga and Mapes* [2012a,b] indicates that slow-moving Matsuno modes [*Matsuno,* 1966] have very different characteristics than rapidly moving modes, suggesting a fundamental difference in the dynamics between the two.

3 Weak temperature gradient approximation

The weak temperature gradient (WTG) approximation is based on the idea that buoyancy anomalies in the tropical atmosphere are rapidly dispersed over a large area by the action of gravity waves, which spread these anomalies over a region comparable in size to the Rossby radius. It has two major applications, first as a theory for balanced disturbances in the tropics [*Charney,* 1963; *Held and Hoskins*, 1985; Sobel *and Bretherton*, 2000; *Sobel et al.*, 2001] and second as a convenient parameterization of the large scale for cloud resolving models in the tropics.

3.1 WTG and tropical dynamics

The most profound difference between the tropics and the middle latitudes is the absence of adiabatic processes leading to strong upward motion in the tropics. Large-scale vertical motion in middle latitudes arises primarily from isentropic upglide in baroclinic environments, a process that is weak in the tropics. Ascent therefore comes largely from moist convection.

Weak horizontal temperature gradients in the tropics can be thought of as a consequence of the small values of the Coriolis parameter there. This is a simple consequence of the thermal wind equation; the horizontal temperature gradient is proportional to the vertical wind shear times the Coriolis parameter. Since the vertical shear is limited by shear instability, an upper limit is imposed on horizontal temperature gradients.

Formally, WTG arises from a scale analysis of the equation for potential temperature θ,

$$\frac{\partial \theta}{\partial t} + \boldsymbol{v}_h \cdot \boldsymbol{\nabla}_h \theta + w \frac{\partial \theta}{\partial z} = H, \tag{6}$$

where $(\boldsymbol{v}_h, w)$ is the wind field, $\boldsymbol{\nabla}_h$ is the horizontal gradient, and H is the heating rate due to turbulent heat fluxes, moist convection, and radiation. If we divide the potential temperature into ambient and perturbation parts $\theta = \theta_0(z) + \theta'$ and then ignore θ' where it occurs in conjunction with θ_0, in agreement with the weak temperature gradient hypothesis, (6) reduces to

$$w\frac{d\theta_0}{dz} = H. \tag{7}$$

Defining $\gamma = d\theta_0/dz$ as the ambient stability, we can solve for the vertical velocity w in terms of γ and the heating rate H:

$$w_{WTG} = \frac{H}{\gamma}. \tag{8}$$

The vertical velocity is given the subscript WTG to emphasize that it represents that ascent required to neutralize heating with vertical advective cooling. With the WTG approximation, all heating is immediately translated into vertical motion.

Sobel et al. [2001] made a formal scale analysis of the equations of motion leading to the above conclusion. The implications of this hypothesis for tropical dynamics are considered below.

3.2 WTG and convection

Cloud resolving models of convection are generally confined to domains that are small compared to the scale of major tropical circulations. Parameterizing the interaction between simulated convection and the large-scale environment is therefore an important issue.

Closed or periodic lateral boundary conditions lead to an important but limited type of model calculation, which, if extended for a long time, results in a statistically steady radiative-convective equilibrium (RCE) state. Since the tropics export only a small fraction of the energy passing through them to middle latitudes [*Peixoto and Oort*, 1992], RCE calculations can be considered a zeroth order approximation to the state of the tropics as a whole, but important differences are expected to exist between such calculations and the mean state of the tropics.

Specifying additional thermodynamic source terms in the model domain to emulate the effects of large-scale flows was proposed by *Randall et al.* [1996] as a solution to the above problem, though precursors to this work go back to *Chang and Orville* [1973], *Soong and Ogura* [1980], and others. Typically, the vertical advection of potential temperature and mixing ratio by the large-scale vertical velocities is applied to produce the desired forcing. Though technically correct, this approach muddies the chain of causality in convection by imposing the vertical velocity. In the deep tropics where balanced lifting is weak, convection itself is generally thought to be responsible for producing the large-scale vertical velocity. The factors controlling the convection must therefore be sought elsewhere.

The WTG parameterization of the large scale addresses this issue. *Raymond and Zeng* [2005] developed a scheme in which the mean temperature profile in the convective domain is relaxed toward a reference temperature profile which is taken to be representative of the clear air

environment surrounding the convection. (Virtual temperature effects are not included in the model.) This relaxation counters the heating due to latent heat release and its turbulent redistribution. The temperature tendency required to effect this relaxation may be thought of as the result of the advection of potential temperature by the WTG vertical velocity. This velocity is considered to be the large-scale vertical velocity resulting from the convective activity. The circulation implied by the WTG vertical velocity, including lateral inflows and outflows demanded by mass continuity, carries water vapor and moist entropy in the model, which results in further modification of the convective environment.

The virtue of WTG lateral boundary conditions is that they provide a parameterization of the large-scale environment in which the convection is embedded that approximately reflects what actually happens in the tropics. Cloud-resolving models with such boundary conditions can therefore be used as a virtual laboratory to test ideas about convective forcing and response. *Wang et al.* [2013] showed that the application of observed time-varying temperature and humidity profiles, surface wind speed, SST, and radiative cooling result in the prediction of a significant fraction of observed rainfall variability by a cloud-resolving model using WTG lateral boundary conditions.

Romps [2012a,b] and *Edman and Romps* [2014] used a related alternative set of lateral boundary conditions which they characterized as the weak pressure gradient (WPG) approximation. These conditions were developed in different contexts by *Kuang* [2008a, 2011] and *Blossey et al.* [2009]. *Romps* [2012a] analyzed the transient response of WTG and WPG to a pulse of heating and found that WTG relaxed short vertical wavelength modes too rapidly, whereas WPG relaxed them too slowly. *Herman and Raymond* [2014] developed a "spectral" version of WTG (SWTG) in which the dependence of relaxation rate on vertical scale lies between WTG and WPG, just matching the results of the linearized analytical model of *Romps* [2012a].

Horizontal temperature gradients are generally weak in the tropical atmosphere except in tropical cyclones. In disturbances such as tropical easterly waves, the gradients are nevertheless large enough to result in temperature anomalies of order 1 K. Such temperature anomalies have enough of an effect on sounding profiles to modulate convective behavior, as we demonstrate below. We hypothesize that this modulation is a key mechanism in tropical atmospheric dynamics.

4 Potential vorticity in the tropics

Given the importance of balanced flow in the tropics, we need to investigate this phenomenon. Potential vorticity dynamics is a compact way of understanding and describing the balanced dynamics of the atmosphere [*McWilliams and Gent,* 1980; *Gent and McWilliams,* 1983a,b,c; *McWilliams*, 1985; *Hoskins et al.*, 1985; *Haynes and McIntyre*, 1987, 1990; *Davis*, 1992; *Raymond*, 1992, 1994]. In middle latitudes the primary balanced process controlling the atmosphere is quasi-geostrophic advection, leading to barotropic and baroclinic energy conversions. In the day-to-day evolution of the mid-latitude atmosphere, diabatic processes, while important, are not dominant.

In the tropics the situation is different. Though barotropic instability is still important, e.g., in the formation of tropical waves and cyclones [*Burpee*, 1972, 1974, 1975; *Norquist et al.*, 1977; *Thorncroft and Hoskins*, 1994a,b; *Molinari et al.*, 1997], baroclinic instability is generally weak to nonexistent, especially for disturbances forming close to the equator, due to the weak horizontal temperature gradients commonly found there. Furthermore, nonlinear balance [*Bolin*, 1955, 1956; *Charney*, 1955, 1962; *Lorenz*, 1960; *McWilliams*, 1985; *Davis*, 1992, *Raymond,* 1992, 1994] must sometimes be used rather than geostrophic balance as a result of the small value of the Coriolis parameter. The efficacy of balanced models in the tropics was demonstrated by *McIntyre and Norton* [2000], at least in the shallow water context.

4.1 Nonlinear balance

As an example of a possible set of idealized quasi-balanced dynamical equations in the tropics, we now examine the nonlinear balance model of *Raymond* [1992, 1994]. In this treatment the horizontal velocity $\boldsymbol{v}_h = (u, v)$ is divided into solenoidal and irrotational parts involving the streamfunction ψ and the velocity potential ϕ

$$u = -\frac{\partial \psi}{\partial y} - \frac{\partial \phi}{\partial x} \qquad v = \frac{\partial \psi}{\partial x} - \frac{\partial \phi}{\partial y} \tag{9}$$

with the fundamental scaling assumption that $|\phi'| \ll |\psi'|$ (the primes indicate that the constant mean value has been subtracted in order to make this relationship unambiguous), though there are circumstances in which this condition can be relaxed. With this scaling assumption as well as the assumption of an equatorial beta plane, the divergence equation simplifies to the nonlinear balance condition

$$\nabla_h^2 \Sigma + \beta \frac{\partial \psi}{\partial y} + 2 \left[\left(\frac{\partial^2 \psi}{\partial x \partial y} \right)^2 - \frac{\partial^2 \psi}{\partial x^2} \frac{\partial^2 \psi}{\partial y^2} \right] = 0 \tag{10}$$

where ∇_h^2 is the horizontal Laplacian and the geostrophic deviation is defined

$$\Sigma = \theta_0 \Pi' - f\psi, \tag{11}$$

with $f = \beta y$ being the Coriolis parameter. The potential temperature $\theta = \theta_0(z) + \theta'$ and Exner function $\Pi = \Pi_0(z) + \Pi'$ are split into ambient and perturbation parts, both of which satisfy the hydrostatic condition

$$\theta_0 \frac{\partial \Pi_0}{\partial z} = -g \tag{12}$$

$$\theta_0 \frac{\partial \Pi'}{\partial z} = \frac{g\theta'}{\theta_0} \tag{13}$$

where g is the acceleration of gravity.

The anelastic mass conservation equation is

$$\frac{\partial \rho_0 w}{\partial z} = \rho_0 \nabla_h^2 \phi \tag{14}$$

where $\rho_0(z)$ is the ambient density profile and w is the vertical velocity. Integrating this in z results in

$$\rho_0 w = \nabla_h^2 \int_0^z \rho_0 \phi dz' \equiv \nabla_h^2 \chi \tag{15}$$

where χ is the vertically integrated velocity potential, so that

$$\phi = \frac{1}{\rho_0}\frac{\partial \chi}{\partial z}. \tag{16}$$

The potential temperature equation may be written

$$\frac{\partial^2 \chi}{\partial x \partial z}\frac{\partial \theta'}{\partial x} + \frac{\partial^2 \chi}{\partial y \partial z}\frac{\partial \theta'}{\partial y} - \nabla_h^2 \chi \left(\gamma + \frac{\partial \theta'}{\partial z}\right) + \rho_0 H = \rho_0 \Theta \tag{17}$$

where H is the heating rate,

$$\gamma = \frac{d\theta_0}{dz}, \tag{18}$$

and

$$\Theta \equiv \frac{\partial \theta'}{\partial t} - \frac{\partial \psi}{\partial y}\frac{\partial \theta'}{\partial x} + \frac{\partial \psi}{\partial x}\frac{\partial \theta'}{\partial y}. \tag{19}$$

This would seem to be a prognostic equation with the time derivative, but it is not; the Exner function perturbation is diagnosed from the nonlinear balance condition (10) and the geostrophic deviation equation (11), and the potential temperature perturbation is then obtained from the hydrostatic equation (12). It is sufficient to compute the time derivative in Θ from backward differencing as demonstrated by *Raymond* [1992], so (17) is actually a diagnostic equation for χ. Once χ is obtained, the unbalanced horizontal wind is computed from (9) and (16) and the vertical velocity from (15).

All we lack is a means of computing the streamfunction ψ to obtain a complete, quasi-balanced solution to the equations of motion, consisting of a balanced horizontal flow plus a secondary circulation incorporating vertical motion. This comes from transporting and inverting the potential vorticity q.

The definition of potential vorticity expands into a (hopefully) elliptic equation involving the streamfunction and the Exner function perturbation:

$$\begin{aligned}\rho_0 q =& \boldsymbol{\zeta} \cdot \boldsymbol{\nabla}\theta \\ =& (f + \nabla_h^2 \psi)\left(\gamma + \frac{\partial \theta'}{\partial z}\right) + \boldsymbol{\zeta}_h \cdot \boldsymbol{\nabla}_h \theta'\end{aligned} \tag{20}$$

where $\boldsymbol{\zeta} = (\boldsymbol{\zeta}_h, \zeta_z)$ is the vector absolute vorticity. Given the scaling assumptions made in this analysis, it is sufficient to approximate the horizontal vorticity $\boldsymbol{\zeta}_h$ by the balanced version of this quantity

$$\boldsymbol{\zeta}_h = -\left(\frac{\partial^2 \psi}{\partial x \partial z}, \frac{\partial^2 \psi}{\partial y \partial z}\right). \tag{21}$$

The flux form of the transport equation is

$$\frac{\partial \rho_0 q}{\partial t} + \boldsymbol{\nabla}_h \cdot (\rho_0 q \boldsymbol{v}_h - \boldsymbol{\zeta}_h H + \gamma \boldsymbol{k} \times \boldsymbol{F}) + \frac{\partial}{\partial z}(\rho_0 q w - H \zeta_z) = 0 \tag{22}$$

where $\boldsymbol{F}$ is the force per unit mass due to friction and turbulent momentum transfer and $\boldsymbol{k}$ is the vertical unit vector. This force is assumed to be "small", so that $\boldsymbol{\nabla}\theta \times \boldsymbol{F}$ is approximated by $\gamma \boldsymbol{k} \times \boldsymbol{F}$. A prognostic equation for the surface potential temperature is needed as well

$$\frac{\partial \theta_S}{\partial t} + \boldsymbol{v}_S \cdot \boldsymbol{\nabla}_h \theta_S = H_S \tag{23}$$

where a subscripted S indicates surface values.

The method for solving this balanced set is as follows:

1. Given q, H, $\boldsymbol{F}$, $\gamma(z)$, $\rho_0(z)$, and θ_S, (10), (13), (20), and (21) are simultaneously solved for ψ, Π', and θ'.

2. The balanced velocities are calculated from ψ.

3. The variable χ is calculated from (17), from which the unbalanced velocities are computed.

4. The potential vorticity and the surface potential temperature are stepped forward in time using (22) and (23) and the whole sequence is repeated.

4.2 Potential vorticity dynamics and WTG

Potential vorticity dynamics simplifies greatly under the weak temperature gradient approximation. The perturbation hydrostatic equation (13) remains as before,

$$\theta_0 \frac{\partial \Pi'}{\partial z} = \frac{g\theta'}{\theta_0}, \tag{24}$$

as does the nonlinear balance condition

$$\theta_0 \nabla_h^2 \Pi' = \nabla_h^2 \left(f\psi \right) - \beta \frac{\partial \psi}{\partial y} - 2 \left[\left(\frac{\partial^2 \psi}{\partial x \partial y} \right)^2 - \frac{\partial^2 \psi}{\partial x^2} \frac{\partial^2 \psi}{\partial y^2} \right]. \tag{25}$$

Dropping θ', the thermodynamic equation (17) simplifies to

$$\rho_0 w_{WTG} = \nabla_h^2 \chi = \rho_0 H / \gamma, \tag{26}$$

which is the same as (8), and the potential vorticity becomes proportional to the absolute vorticity

$$\rho_0 q = \zeta_z \gamma = (f + \nabla_h^2 \psi)\gamma. \tag{27}$$

Similarly, the potential vorticity governing equation becomes the flux form of the absolute vorticity equation

$$\frac{\partial \zeta_z}{\partial t} + \boldsymbol{\nabla}_h \cdot (\zeta_z \boldsymbol{v}_h - \boldsymbol{\zeta}_h w_{WTG} + \boldsymbol{k} \times \boldsymbol{F}) = 0 \tag{28}$$

with the horizontal velocity $\boldsymbol{v}_h$ derived from ψ and χ as before

$$u = -\frac{\partial \psi}{\partial y} - \frac{1}{\rho_0}\frac{\partial^2 \chi}{\partial x \partial z} \qquad v = \frac{\partial \psi}{\partial x} - \frac{1}{\rho_0}\frac{\partial^2 \chi}{\partial y \partial z}. \tag{29}$$

The fact that θ' remains in (24) shows why WTG is called the "weak temperature gradient" approximation rather than the "zero temperature gradient" approximation. The potential temperature perturbation must be non-zero in the hydrostatic equation in order for baroclinic flows to occur; if it is zero, then $\partial \Pi'/\partial z = 0$ and the flow is completely barotropic, not admitting any vertical motion. This is the only place in the governing equations that θ' occurs as the first non-vanishing term involving the potential temperature. As we shall see, θ' is crucially important to the structure of tropical convection, even though it is generally "small".

4.3 Potential vorticity inversion at equator

Though balanced models are more useful in the tropics than one might naively expect, the zonally symmetric flow at and near the equator still presents difficulties. As *Raymond* [1994] pointed out, there exist zonally symmetric Kelvin modes that are balanced, but which have no potential vorticity signature on isentropic surfaces. As with any Kelvin modes, these disturbances decay rapidly in amplitude away from the equator with a decay scale that is proportional to their vertical scale. Shallow modes of this type are problematic in particular, as the horizontal decay scale is so small that they become essentially zero at high latitudes and are therefore unconstrained by high-latitude boundary conditions. Furthermore, since their potential vorticity structure is invisible on isentropic surfaces, they are not controlled by potential vorticity dynamics. They therefore exist outside of the balanced dynamics paradigm, even though their zonal flows are in geostrophic balance with the pressure field.

Raymond [1994] concluded that zonally symmetric Kelvin modes are controlled by meridional and vertical fluxes of zonal momentum. Thus, for any global balanced model, an additional set of equations outside of the balanced context must be included to account for the dynamics of these modes. The stratospheric jet in the quasi-biennial oscillation [*Lindzen and Holton*, 1968; *Holton and Lindzen*, 1972] appears to be a candidate for a disturbance of this type.

5 Thermodynamic control of tropical convection

The question remains as to what controls convection when the cooperative intensification mechanism of Ooyama does not apply. In pursuing this question we forego any attempt to construct a simplified picture of chaotic mesoscale dynamics. Instead we focus on averages over space and time scales on which thermodynamic factors place significant constraints on convection. Two approaches to the problem employing the concept of quasi-equilibrium are first outlined. Then a view of convective control arising from observations of convection in potential tropical cyclone precursors is presented. Finally, the role of gross moist stability is discussed.

5.1 Boundary layer quasi-equilibrium

Basic physics indicates that convection can occur only when there is convective instability. In the case of moist convection, positive parcel buoyancy can often be acquired only by mechanically lifting a boundary layer parcel through a capping layer where it has negative buoyancy until it reaches the level of free convection. This is the conditional instability mechanism. The smaller the so-called convective inhibition (CIN), which is the specific kinetic energy needed to perform this lifting, the more readily this capping layer is penetrated. Further ascent depends on the continued maintenance of positive buoyancy in the face of entrainment of surrounding environmental air.

Over warm tropical oceans, the thermodynamic sounding is typically conditionally unstable, suggesting that the capping layer exercises control over the initiation of deep convection. *Emanuel* [1995] and *Raymond* [1995] developed theories of convective initiation based on the factors governing conditional instability. Given the value of saturated moist entropy s_t in the capping layer (the threshold moist entropy) and the boundary layer moist entropy s_b, the upward convective mass flux m_u is expressed by *Raymond* [1995] in terms of $s_b - s_t$,

$$m_u = C(s_b - s_t), \tag{30}$$

where C is a constant. Balanced dynamics controls s_t, at least in time averages over intervals exceeding T_B.

The factors controlling the boundary layer entropy s_b are primarily the surface moist entropy flux and downdrafts from the free troposphere into the boundary layer, with a small contribution from radiation. The downdrafts at the top of the boundary layer are some combination of turbulent entrainment and evaporatively driven downdrafts from convection. We neglect turbulent entrainment for now for simplicity, and assume that the downdraft mass flux is some fraction α of the updraft mass flux

$$m_d = \alpha m_u. \tag{31}$$

The entropy tendency in a boundary layer column may be written

$$\frac{d\rho_b b s_b}{dt} = -\rho_b b s_b \boldsymbol{\nabla}_h \cdot \boldsymbol{v}_h - m_u s_u + m_d s_d + F_s - F_t + \rho_b b R \tag{32}$$

where ρ_b is the (constant) air density in the boundary layer, b is its (fixed) depth, entropy values in the updraft and downdraft mass fluxes are s_u and s_d, $\boldsymbol{v}_h$ is the horizontal wind in the boundary layer, R is the specific radiative source of moist entropy, and $F_s - F_t$ is the surface entropy flux minus the upward turbulent entropy flux at the top of the boundary layer.

Mass continuity in the boundary layer takes the form

$$b\rho_b \boldsymbol{\nabla}_h \cdot \boldsymbol{v}_h + m_u - m_d = 0. \tag{33}$$

Multiplying this by s_u and adding to (32) results in

$$\frac{d\rho_b b s_b}{dt} = \rho_b b(s_u - s_b)\boldsymbol{\nabla}_h \cdot \boldsymbol{v}_h - m_d(s_u - s_d) + F_s - F_t + \rho_b b R. \tag{34}$$

If we set $s_u = s_b$, then (34) reduces to

$$m_u = \frac{m_d}{\alpha} = \frac{F_s - F_t + \rho_b b R}{\alpha(s_b - s_d)} \tag{35}$$

in the equilibrium case in which the time derivative is zero. Strong surface fluxes and weak downdraft fluxes of moist entropy thus favor strong updraft production.

Raymond [1995] estimated that the time scale T_{BLQ} for boundary layer quasi-equilibrium to become established is typically half a day over warm tropical oceans with normal undisturbed surface winds. If the winds are stronger, then the time to equilibrium is correspondingly reduced. This time scale is not so different from the time scale T_B for the establishment of balance in quiescent tropical conditions.

Thayer-Calder and Randall [2015] found in a cloud-resolving model that the turbulent flux of entropy at the top of the sub-cloud layer tends to exceed that produced by convective downdrafts. However, recent work has tended to apply boundary layer quasi-equilibrium to a thicker layer, such as the full planetary boundary layer, as discussed below, and it is unclear whether Thayer-Calder and Randall's criticism extends to that case.

5.2 Tropospheric quasi-equilibrium

Boundary layer quasi-equilibrium is an incomplete theory of convection, as it addresses only the upward convective mass flux leaving the boundary layer. What happens to the updraft after this is left open, as are the factors controlling downdraft characteristics as parameterized by α and s_d. A more ambitious but still incomplete theory is that of full tropospheric convective quasi-equilibrium.

Arakawa and Schubert [1974] introduced the idea of convective quasi-equilibrium. In their model, a balance exists between factors destabilizing the free troposphere and the convection itself, which is considered to stabilize the environment. In equilibrium, the environment sits on the edge of instability in their model and the amount of convection is that required to just balance destabilization. This equilibrium is possible only if the time constant for convective stabilization is much shorter than those of destabilizing processes. In the Arakawa-Schubert model, a distribution of convective plumes with different detrainment rates is specified so as to just match the profiles of stabilization and destabilization.

The algorithm for matching the plume spectrum to the destabilization profile in the Arakawa-Schubert scheme is computationally expensive and difficult to code. *Moorthi and Suarez* [1992] created a "relaxed" version of the Arakawa-Schubert scheme that overcomes these problems. *Cheng and Arakawa* [1997] introduced convective downdrafts into the Arakawa-Schubert scheme as well.

A potentially serious problem of the Arakawa-Schubert model is that large-diameter, weakly entraining plumes tend to crowd out smaller, more strongly entraining plumes, with deleterious effects under certain circumstances [*Tokioka et al.*, 1988]. This problem was solved by introducing a minimum entrainment rate that decreases as the boundary layer depth increases.

Perhaps the most general expression of the convective quasi-equilibrium hypothesis is that of *Emanuel et al.* [1994]. The essence of their argument is that convection controls the virtual temperature profile of convective regions in the tropics by the reasoning expressed in the context of the Arakawa-Schubert model. In the "strict quasi-equilibrium" version of their hypothesis, convection instantly drives the troposphere to moist neutrality. In the simplest version of strict convective quasi-equilibrium, the moist-neutral profile has constant tropospheric saturated moist entropy (or saturated equivalent potential temperature) equal to the boundary layer moist entropy. The boundary layer entropy is set by the processes discussed in the section on boundary layer quasi-equilibrium, though the details are different because the capping layer itself is considered to be malleable. *Emanuel et al.* [1994] also investigate the effect of introducing a small lag (of order 1 hr) in the convective equilibration process. In this case, large-scale waves are damped by convection in the absence of external energy sources.

It is hard to argue that the tropical atmosphere sits on the edge of zero convective available potential energy (CAPE), as would be expected in the simplest convective quasi-equilibrium models, in spite of the best efforts of *Xu and Emanuel* [1989]. *Brown and Bretherton* [1997], *Sobel et al.* [2004], and *Lin et al.* [2015] showed that the behavior of the tropical atmosphere is inconsistent with this picture. In a more complex model such as that of *Arakawa and Schubert* [1974], the neutral sounding depends on the vertical profile of humidity as well as the spectrum of convective plumes excited by destabilization, so the analyses of *Brown and Bretherton* [1997], *Sobel et al.* [2004], and *Lin et al.* [2015] are possibly less applicable to such models. However, their criticisms are likely to apply to simpler quasi-equilibrium models such as that of *Neelin and Zeng* [2000] and *Zeng et al.* [2000].

Kuang [2008a] indicates, on the basis of cloud-resolving numerical simulations embedded in simplified large-scale waves, that a strong correlation between boundary layer moist entropy and the virtual temperature profile exists only in the lower troposphere. *Khouider and Majda* [2008] make a similar assumption in their linearized model. *Raymond and Herman* [2011] argue that rapid phase change is required to produce quasi-equilibrium behavior, a process that is limited to the lower troposphere. Basically, convection can't transport sensible heat rapidly enough to the upper troposphere to enforce quasi-equilibrium on a short time scale according to theoretical and numerical modeling. These results suggest that full tropospheric convective quasi-equilibrium does not occur in the tropics, but may exist in the lower troposphere.

Raymond et al. [2003] showed that the observed behavior of deep convection over tropical oceans is more consistent with boundary layer quasi-equilibrium modified to include the full planetary boundary layer (1 km or more in depth) as the source region for convective updrafts rather than just the subcloud layer. The inhibition layer therefore becomes centered near 1.5 km or above. *Sobel et al.* [2004] obtained similar results. *Raymond et al.* [2003] called this deep convective inhibition (DCIN). Since DCIN is conceptually similar to lower tropospheric CAPE with the exception of a sign, boundary layer quasi-equilibrium begins to look more like lower tropospheric quasi-equilibrium with this modification. Given the above results, there appears to be broad convergence on the idea that the lower tropospheric virtual temperature profile plays a critical role in controlling deep tropical convection.

Two additional comments may be made regarding the idea of convective quasi-equilibrium. First, *Mapes* [2000] suggests on the basis of a simplified model that even an apparently well-justified quasi-equilibrium model can give very different results for tropical waves than an equivalent non-equilibrium treatment, for example, by not dispensing with the time derivative in the boundary layer entropy governing equation (32). However, this complication may be limited to the unbalanced, rapidly moving wave disturbances considered in that paper. Slowly evolving, quasi-balanced systems may be less sensitive to this issue.

There may also be a competition between the respective tendencies of convective adjustment and large-scale dynamical adjustment (i.e, relaxation to a balanced state) to establish the virtual temperature profile. Given the results of *Kuang* [2008a,b] and *Raymond and Herman* [2011], it seems likely that large-scale dynamics wins in the upper troposphere. The most likely battleground is the lower troposphere, where convective adjustment processes tend to occur relatively rapidly. However, *Raymond* [2012] shows that the virtual temperature profile in the intense convective environment of developing tropical cyclones is nearly in dynamical balance with the vorticity field everywhere above the boundary layer, suggesting that dynamical adjustment dominates even in the lower troposphere.

5.3 Control of convection by vorticity and SST

Results from recent field programs studying tropical cyclogenesis, namely the Tropical Cyclone Structure experiment [TCS-08; *Elsberry and Harr*, 2008] and the Pre-Depression Investigation of Cloud Systems in the Tropics [PREDICT; *Montgomery et al.*, 2012], have led to significant insight into the factors controlling deep convection in the tropics. These results are reported by *Raymond et al.* [2011], *Gjorgjievska and Raymond* [2014], and *Raymond et al.* [2014]. We use here the windowed dropsonde analyses derived by *Gjorgjievska and Raymond* [2014] for PREDICT and TCS-08 to illustrate the mechanisms uncovered in these studies. But first we introduce some ideas derived from theory and modeling.

Raymond [2000] proposed a simple model of convective precipitation based on the hypothesis that the rainfall rate scales inversely with the vertically integrated saturation deficit of the atmosphere. This hypothesis was verified qualitatively for convection over tropical oceans by *Bretherton et al.* [2004]. Figure 2 of *Raymond et al.* [2007] showing saturation fraction (roughly speaking, one minus saturation deficit) versus rainfall rate, reproduced here as figure 2, shows similar results using a different data set. Saturation fraction is defined as

$$S = \int r dp \Big/ \int r^* dp \tag{36}$$

where the pressure integrals of mixing ratio r and saturation mixing ratio r^* are taken over the full troposphere.

The key assumption in *Raymond* [2000] is that the gross moist stability [GMS; *see Raymond et al.*, 2009] of the atmosphere, defined as the vertically integrated lateral export of moist entropy divided by the integrated lateral import of moisture, can be specified a priori. Taking into account both the moisture and moist entropy budgets of a test volume in the atmosphere allows the time-dependent evolution of the saturation deficit and rainfall rate to be computed

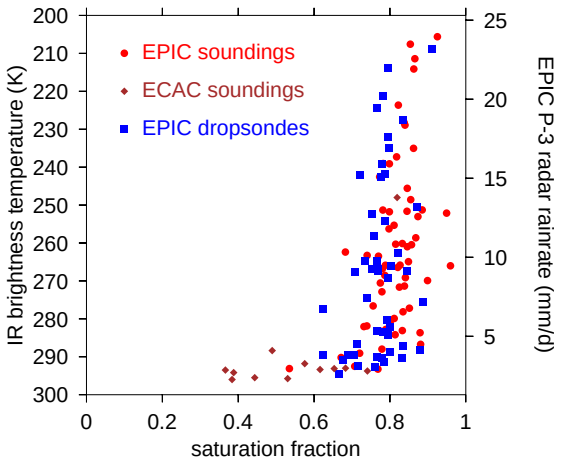

Figure 2: Infrared brightness temperature and airborne radar rainfall rate vs. saturation fraction in the eastern tropical Pacific and southwest Caribbean. After figure 1 in *Raymond et al.* [2009].

under these conditions. As long as the GMS is positive, the saturation deficit and rainfall rate evolve toward equilibrium values. In cases with small GMS, this evolution is particularly rapid, with higher equilibrium rainfall rates also exhibited.

In reality, the GMS is not constant, but varies with environmental conditions. To seek a truly prognostic theory of equilibrium rainfall, one must determine how the GMS of convection is controlled by the thermodynamic environment. By "thermodynamic environment", we mean the temperature and humidity profiles in which convection is embedded, the SST, and the surface fluxes of sensible and latent heat. The environmental wind profile, in particular the wind shear, should also in principle be included as a control factor, but we have yet to consider the effects of this quantity and shall discuss only the purely thermodynamic factors here. *Anber et al.* [2014] have begun to explore the effects of shear on the statistics of convection.

Raymond and Zeng [2005] showed results from cloud resolving model simulations that are similar to those seen in figure 2. These simulations used the WTG parameterization of the large scale environment. Figure 3 shows more recent calculations in which the mean saturation fraction in the convective domain and in the reference profile are plotted versus the mean rainfall rate in approximately 100 SWTG numerical simulations of convection. These two-dimensional simulations are forced by a diverse set of surface fluxes as well as perturbations in temperature ($\approx \pm 1$ K) and humidity ($\approx 10\%$) to the initial SWTG reference profiles. The initial profiles were obtained as averages of profiles from a long-term radiative-convective equilibrium calculation, as was done by Raymond and Sessions (2007). Horizontal and vertical resolutions are 1 km and 0.25 km and the domain size is 192 km by 20 km. The assumed relaxation scale is $L = 150$ km, which corresponds to a fundamental mode relaxation time of about 1 hr [*see Herman and Raymond*, 2014].

The domain-mean and reference profile saturation fractions in figure 3 differ significantly, with almost no correlation between the two. Furthermore, the domain-mean humidity more closely resembles observations shown in figure 2 than does the reference profile humidity; it

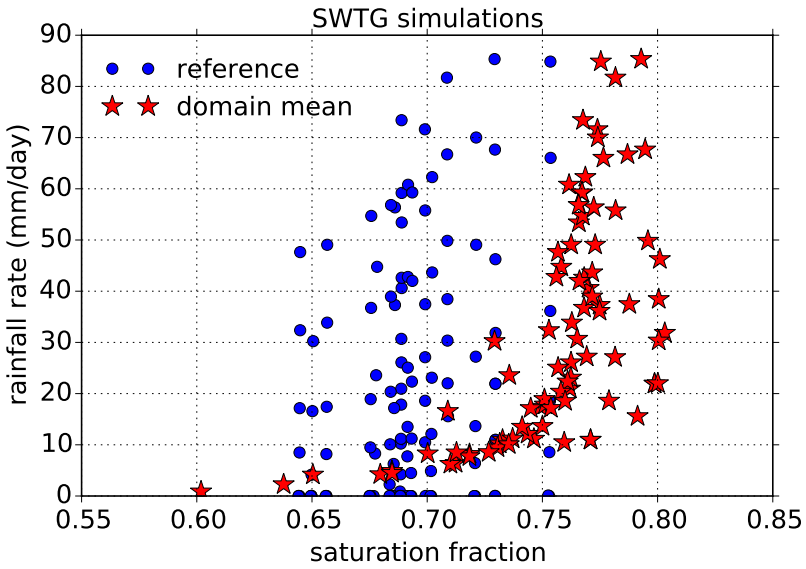

Figure 3: Scatter plot of saturation fraction vs. mean rainfall rate in SWTG simulations. The red stars indicate the saturation fraction in the convective domain while the blue circles indicate this quantity in the reference profile.

is unclear as to whether the latter corresponds to anything observable. Since the moisture in the immediate convective environment, as represented by the domain-mean values in figure 3, is not closely related to the reference profile of humidity, it cannot be an environmental predictor of convection, but instead must be largely a result of the convection itself. We therefore must seek the factors controlling convection from the other available variables.

We now turn to our observational results. Figure 4 shows the sum of the calculated moisture convergence and the surface evaporation rate (equal to the rainfall rate in the steady state) versus the saturation fraction for the 37 TCS-08 and PREDICT field case studies. The horizontal axis covers a more limited range than that in figure 2 and the maximum rainfall rates are higher, but the two results are otherwise similar. Further examination of our data set shows that the rainfall rate and related quantities such as the vertical mass flux have at best very weak correlations with any plausible potential environmental controls. Variations in the saturation fraction account for only about 20% of the variance in rainfall in our data. This is most likely due to the fact that our observations are snapshots that don't capture average precipitation rates and mass flux profiles.

To make further progress we assume that the saturation fraction itself is a surrogate for average precipitation rate and investigate the factors that control the saturation fraction. This path is more fruitful than seeking correlations with precipitation directly, due to the factors discussed above.

The remaining predictive variables available to us are variability in the tropospheric temperature, the surface heat and moisture fluxes, and the SST. We represent the fluxes in

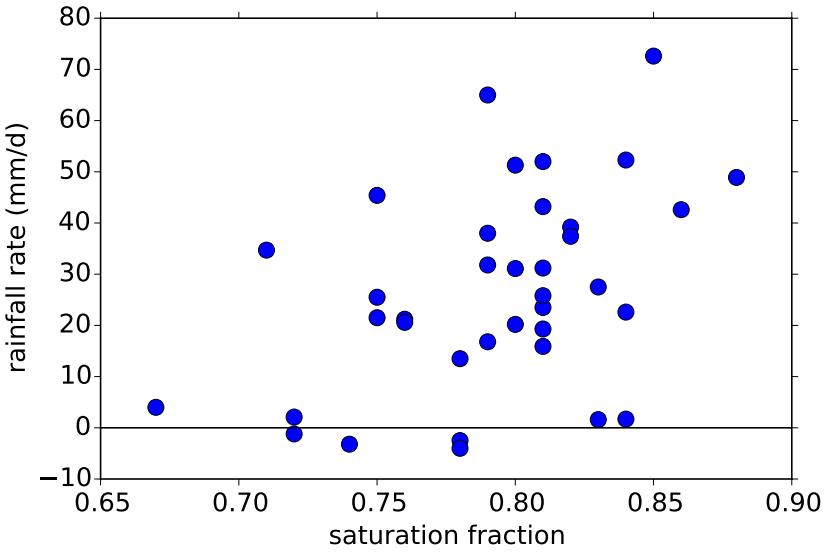

Figure 4: Rainfall rate (actually, moisture convergence plus surface evaporation rate) as a function of saturation fraction for all TCS-08 and PREDICT case studies.

terms of surface evaporation rate and the surface flux of moist entropy. Unsurprisingly, the evaporation rate and the moist entropy flux are highly correlated due to the weakness of surface sensible heat fluxes over warm tropical oceans, so we need only choose one. We often expect that dependence on SST is subsumed by the dependence on surface heat fluxes, but there are situations where this is not true. The available predictive thermodynamic quantities are thus variability in the temperature profile, in the surface evaporation rate, and in the SST. Due to the powerful tendency for buoyancy anomalies to be redistributed by gravity waves, the domain-mean and reference temperature profiles differ much less than the humidity profiles in our SWTG calculations, indicating that virtual temperature profiles measured in convective regions are more indicative of the "undisturbed" environment than are humidity profiles.

A common pattern of variability in the tropical temperature profile associated with enhanced deep convection is cooling in the lower troposphere and warming in the upper troposphere. For instance, this occurs in African easterly waves [*Reed et al.*, 1977; *Thompson et al.*, 1979; *Cho and Jenkins*, 1987; *Jenkins and Cho*, 1991] and developing tropical cyclones [*Bister and Emanuel*, 1997; *Raymond et al.*, 1998; *Raymond et al.*, 2011; *Gjorgjievska and Raymond*, 2014]. A perturbation of this type reduces the moist convective instability of the middle troposphere. A measure of variability of this type is represented by the instability index [*Raymond et al.*, 2011]

$$I = s^*_{low} - s^*_{mid} \tag{37}$$

where s^*_{low} is the saturated moist entropy averaged over the $[1, 3]$ km layer while s^*_{mid} is the same variable averaged over $[5, 7]$ km. The saturated moist entropy is a function only of the

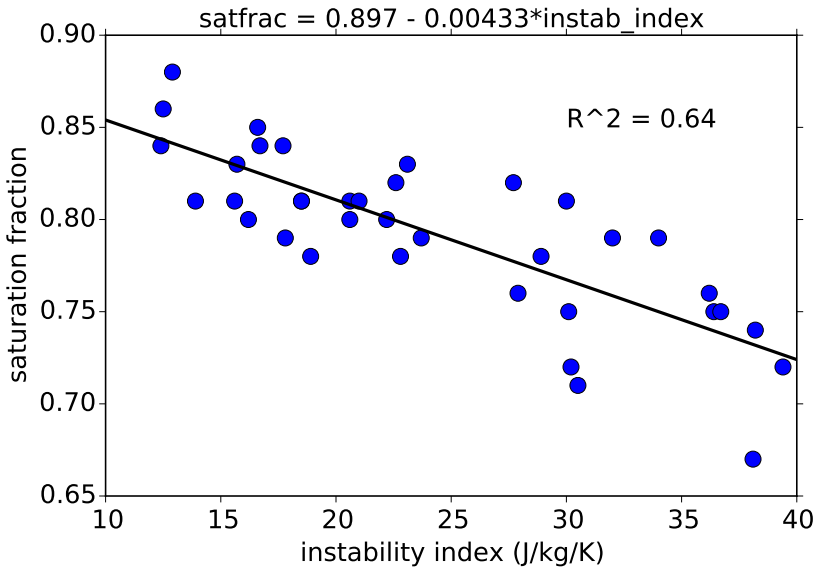

Figure 5: Scatter plot of saturation fraction vs. instability index in the observational data set along with the linear regression line. The variability in the instability index explains 64% of the variance of saturation fraction.

temperature and pressure, which means that at a given pressure level it is a surrogate for the temperature. Furthermore, $I = 0$ when the moist convective (not conditional) instability is zero. Thus, larger values of I indicate larger moist convective instability. The instability index is related to CAPE when the boundary layer moist entropy is in equilibrium with the saturated moist entropy in the lower troposphere, as discussed in section 5.1.

A curious result of our analysis is that the instability index is inversely correlated with the saturation fraction, as shown in figure 5. The correlation becomes more strict at higher saturation fractions. This correlation is in agreement with the frequently reported result that CAPE and relative humidity are inversely related in the tropical atmosphere [*see e.g., Ramage*, 1971; *Williams et al.*, 1992; *Brown and Bretherton*, 1997]. *Singh and O'Gorman* [2013] proposed that this correlation is related to the fact that convective plumes are evaporatively cooled more by the entrainment of dry air compared to moist air. For a given entrainment rate, plumes penetrating through dry air therefore need greater moist convective instability to maintain positive buoyancy than do plumes in a moist environment. The fact that vertical velocities in tropical convection are typically rather small [*e.g., LeMone and Zipser*, 1980; *Zipser and LeMone*, 1980], at least in the lower troposphere, suggests that a feedback mechanism maintains the tropical environment near this critical instability value. Perhaps decelerating plumes deposit their moisture in the dry layer if the atmosphere is too dry, thus moistening it, whereas if it is too moist, vigorous plumes produce an excess of rain, which dries the atmosphere. We denote this putative feedback mechanism "moisture quasi-equilibrium".

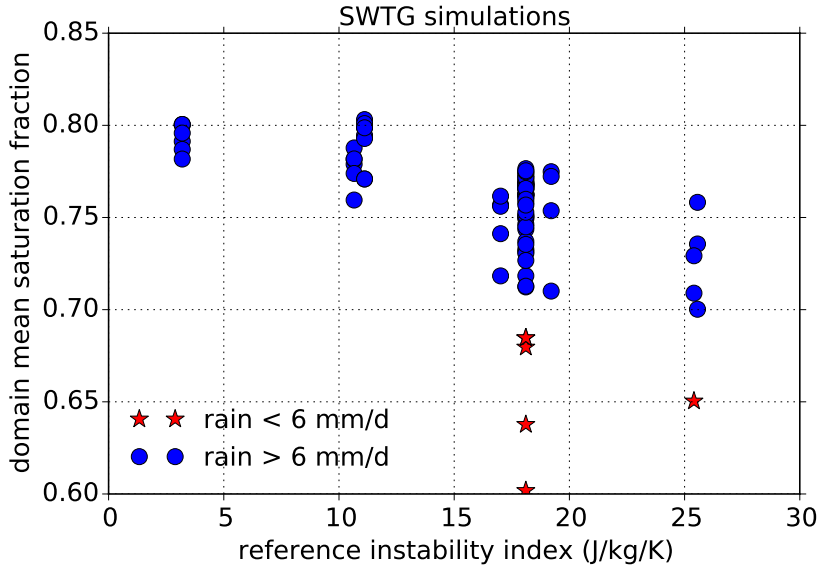

Figure 6: Convective domain saturation fraction vs. reference profile instability index in SWTG cloud model simulations. Those with rainfall rate less than 6 mm/day are distinguished from those with greater rainfall rates. The discrete values of instability index reflect the limited set of reference temperature profiles used in the simulations.

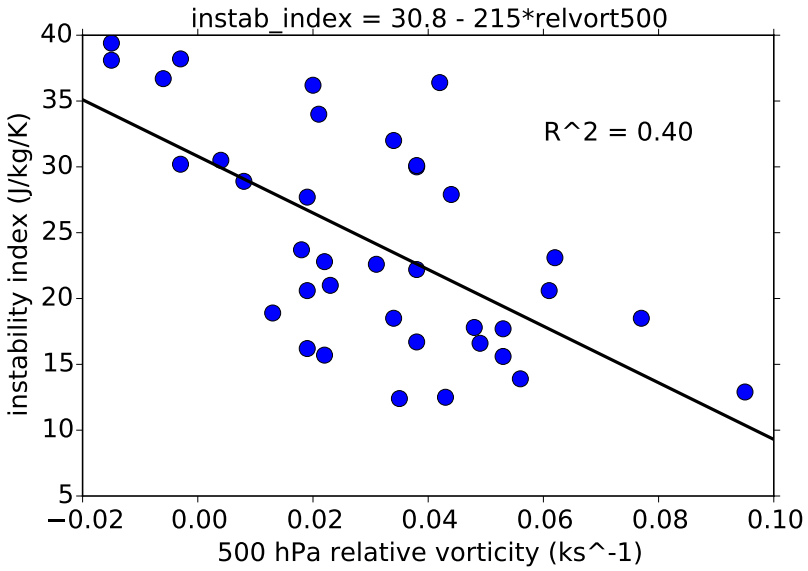

Figure 7: Scatter plot of instability index vs. 500 hPa average relative vorticity for our case studies.

Our recent SWTG convective simulations, as illustrated in figure 6, show qualitative behavior similar to that seen in observations (figure 5). The range of instability indices explored is somewhat different in the two figures, and the saturation fractions corresponding to particular values of instability index are somewhat less. This likely reflects differences between the modeled and real-world thermodynamics and cloud physics in these two cases. The most significant difference is that the model results show smaller values of saturation fraction for lower rainfall rates. As the observations were biased toward convectively disturbed regions, the lack of such low saturation fraction cases in the observations is to be expected.

Raymond et al. [2011] and *Gjorgjievska and Raymond* [2014] hypothesized that the balanced temperature dipole observed in the presence of a mid-tropospheric vortex has a profound effect on the form of convection in this environment, in particular, making the vertical convective mass flux profile more bottom-heavy. *Raymond* [2012] showed that the observed cool anomaly below a mid-level vortex and the warm anomaly above are in non-linear balance with the vortex in a few observed cases, suggesting that this dipole is not a direct effect of the convection itself, but a consequence of the vorticity pattern in the atmosphere. The convection can affect the vorticity distribution, but on a time scale longer than the typical convective life cycle. Thus, the temperature dipole does not co-vary with the convection, but is actually a convective predictor, as suggested by our SWTG modeling.

Given the above hypothesis, the instability index, which as noted above is an indicator of a tropospheric temperature dipole, should be negatively correlated with the vorticity at middle levels. Our set of case studies indeed confirm this behavior, as illustrated in figure 7. The fraction of variance explained is 40%, which is not large, but is nevertheless

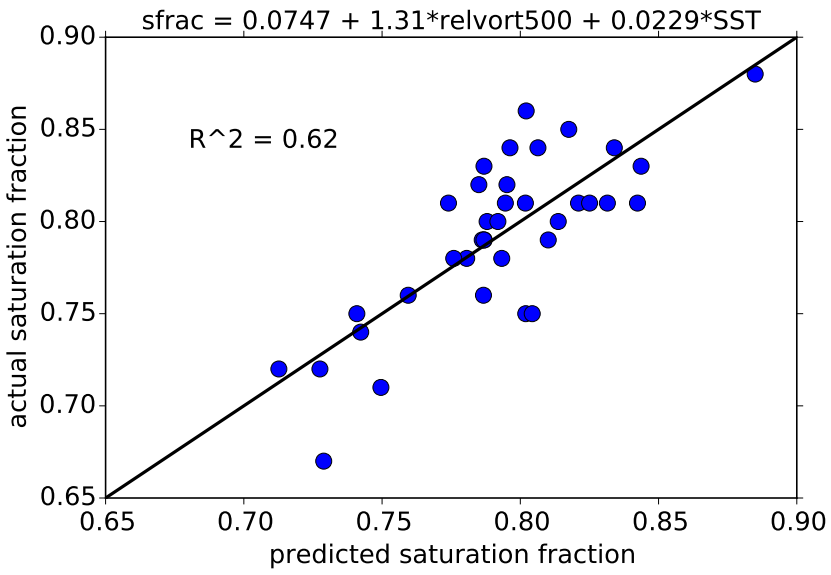

Figure 8: Actual vs. predicted saturation fraction as a function of 500 hPa vorticity (ks^{-1}) and sea surface temperature (degrees Celsius). 62% of the variance in saturation fraction is explained by these two variables.

very suggestive. Thus the arrow of causality likely points from mid-level vorticity to the tropospheric temperature profile to saturation fraction to rainfall rate in this data set.

We also examine the direct correlation between saturation fraction and and mid-level vorticity. A striking positive correlation exists between these quantities, with 52% of the variance in saturation fraction explained by the 500 hPa vorticity. There is negligible correlation between saturation fraction and surface evaporation rate, but 11% of the variance in this quantity is explained by variations in the SST. The mid-level vorticity and SST together explain 62% of the variance in saturation fraction in a multiple linear regression, which is only slightly less than the sum of the individual variances, indicating that these quantities are largely independent. Figure 8 shows a scatter plot of actual versus predicted saturation fraction, with the diagonal line being the regression line.

Together, these modeling and observational results strongly suggest that convection and precipitation are jointly controlled by the strength of the mid-level vorticity and the SST, though confidence in the SST contribution is somewhat reduced, due to its small contribution to the variance in the sample. The causal path between vorticity and convection involves perturbations in the tropospheric temperature profile associated with the balanced response to a mid-level vortex which result in changes in the saturation fraction that come from the moisture quasi-equilibrium process. The SST likely plays a role in this via its effect on the buoyancy of air parcels ascending from the boundary layer. Increases in saturation fraction result, on the average, in increases in precipitation rate.

5.4 Gross moist stability

The previous section dealt with the relationship between the convective environment and precipitation. We now consider the relationship between the environment and other observed convective characteristics. The gross moist stability provides a window into these issues.

There are many ways to define gross moist stability. We use the normalized gross moist stability [*Raymond and Sessions*, 2007], which we define here as

$$\Gamma = -\frac{T_R[\boldsymbol{\nabla} \cdot (\rho s \boldsymbol{v})]}{L[\boldsymbol{\nabla} \cdot (\rho r \boldsymbol{v})]} \tag{38}$$

where the divergence is three-dimensional and the square brackets indicate a vertical integral from the surface to a level in the upper troposphere which may not quite reach cloud top. The air density is ρ, the specific moist entropy is s, the water vapor mixing ratio is r, and the three-dimensional velocity is $\boldsymbol{v}$. Constant reference values are $T_R = 300\,\mathrm{K}$ and $L = 2.83 \times 10^6\,\mathrm{J/kg}$ (sum of latent heats of condensation and freezing). Implicit horizontal averaging is assumed in the numerator and denominator of this equation, corresponding to averaging made over a region of gridded observational data.

The reason for using a limited vertical domain is that research aircraft generally cannot reach the elevation of the highest cloud tops in the tropics. Use of the three-dimensional divergence means that fluxes out of the top of the observed domain are accounted for, albeit in a possibly incomplete fashion, as the eddy fluxes out of the domain top associated with convective towers are generally not measured. However, at these altitudes the eddy flux of water vapor is negligible, so that the moisture convergence in the denominator is well represented. The entropy fluxes in the numerator are somewhat more problematic, though this is possibly not a large issue as the entropy at high elevations is essentially the dry entropy. The tendency of updrafts at high levels to overshoot and subside suggests that to zeroth order, the associated dry entropy fluxes may largely counterbalance each other.

The vertically integrated moist entropy budget may be written

$$\frac{\partial[\rho s]}{\partial t} + [\boldsymbol{\nabla} \cdot (\rho s \boldsymbol{v})] = F_s - R \tag{39}$$

where F_s is the surface moist entropy flux and R is the vertically integrated radiative entropy sink. A similar equation may be written for the water vapor mixing ratio:

$$\frac{\partial[\rho r]}{\partial t} + [\boldsymbol{\nabla} \cdot (\rho r \boldsymbol{v})] = E - P \tag{40}$$

where E is the surface evaporation rate and P is the precipitation rate. In steady state, the precipitation rate thus becomes

$$P = E - [\boldsymbol{\nabla} \cdot (\rho r \boldsymbol{v})]. \tag{41}$$

It is customary to split the numerator of the NGMS into parts associated with the horizontal and vertical advection of moist entropy, e.g., *Back and Bretherton* [2006]. Using the anelastic

mass continuity equation $\boldsymbol{\nabla} \cdot (\rho \boldsymbol{v}) = 0$ and splitting the advection term into horizontal and vertical parts, (39) may be rewritten

$$\frac{\partial [\rho s]}{\partial t} = - \left[\rho \boldsymbol{v}_h \cdot \boldsymbol{\nabla}_h s\right] - \left[\rho w \frac{\partial s}{\partial z}\right] + F_s - R. \tag{42}$$

Unfortunately, dropsonde observations are unable to resolve individual convective cells, so the averaging of observed vertical advection underestimates the effects of convective-scale advection. An alternate way of splitting the entropy divergence is to divide the system-relative horizontal wind into two pieces $\boldsymbol{v}_h = \boldsymbol{v}_0 + \boldsymbol{v}_r$ where $\boldsymbol{v}_0(z)$ is the horizontal average of the system-relative wind and $\boldsymbol{v}_r$ is the deviation from this average. We include the latter part with the resolved-scale vertical advection, resulting in

$$\frac{\partial [\rho s]}{\partial t} = -A_h - A_v + F_s - R \tag{43}$$

where

$$A_h = \left[\rho \boldsymbol{v}_0 \cdot \boldsymbol{\nabla}_h s\right] \qquad A_v = \left[\rho \boldsymbol{v}_r \cdot \boldsymbol{\nabla}_h s + \rho w \frac{\partial s}{\partial z}\right]. \tag{44}$$

The first term is interpreted as the ventilation by the system-relative mean wind profile, whereas the second term includes the effects of lateral entrainment and detrainment associated with the vertical wind. In what follows, we use A_h and A_v as defined by (44).

Raymond [2013] derived an accurate expression for the specific moist entropy including the effects of the ice phase. A simple, approximate expression for this variable is

$$s \approx C_p \ln \theta + \frac{Lr}{T_R} \tag{45}$$

where C_p is the specific heat of air at constant pressure, θ is the potential temperature, and r is the water vapor mixing ratio. This equation is useful because it shows that variations in the entropy at constant potential temperature are equivalent to variations in the mixing ratio. Thus, if the temperature profile doesn't change much, the budget of entropy is essentially a budget of water vapor. This is an important result, because it allows us to determine whether the convective column is moistening or drying without the difficulty of computing this tendency as a small residual of the moisture convergence and precipitation in the moisture budget.

The vertical convective mass flux profile is also derived from our analysis of observations [*Gjorgjievska and Raymond,* 2014]. We find it useful to examine averages of the vertical mass flux over the vertical ranges $[3, 5]\,\mathrm{km}$ (M_{lo}) and $[7, 9]\,\mathrm{km}$ (M_{hi}) in elevation. The difference between these two quantities, $M_{dif} = M_{hi} - M_{lo}$, is also useful.

Figure 9 shows a scatter plot of M_{lo} versus the inferred precipitation rate P. As expected, these two quantities are highly correlated, since the moisture convergence is closely related to the low-level mass convergence, and hence the vertical mass flux at the top of the moist layer.

As figure 10 shows, M_{hi} is not well correlated with M_{lo}, and hence with the precipitation rate. In most cases $M_{hi} > M_{lo}$. However, M_{dif} is well correlated with A_v as shown in figure

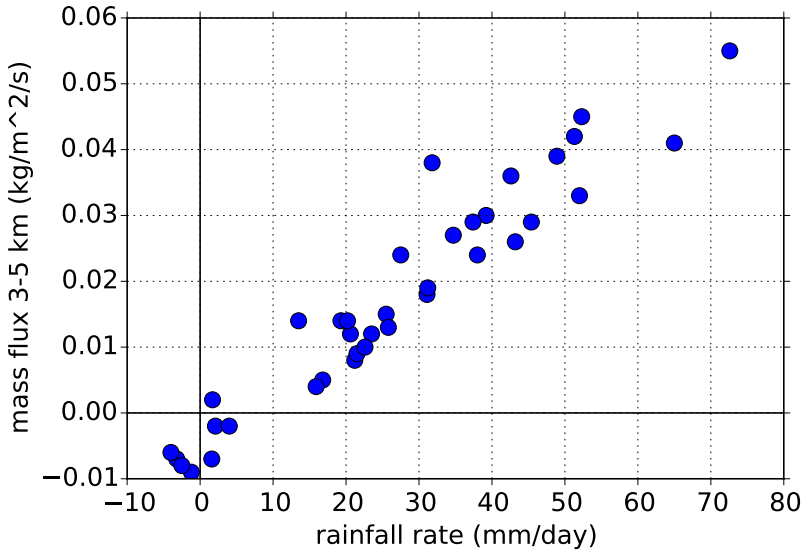

Figure 9: Scatter plot of vertical mass flux in the $[3, 5]$ km layer vs. the inferred precipitation rate.

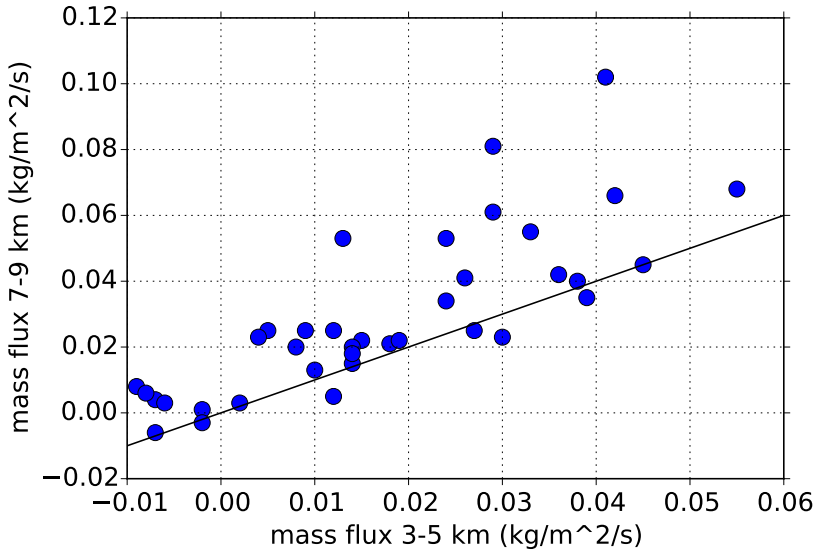

Figure 10: Scatter plot of vertical mass flux in the $[7, 9]$ km layer vs. its value in the $[3, 5]$ km layer. The upper level mass flux exceeds the lower level value for points above the slanted line, where $M_{hi} = M_{lo}$.

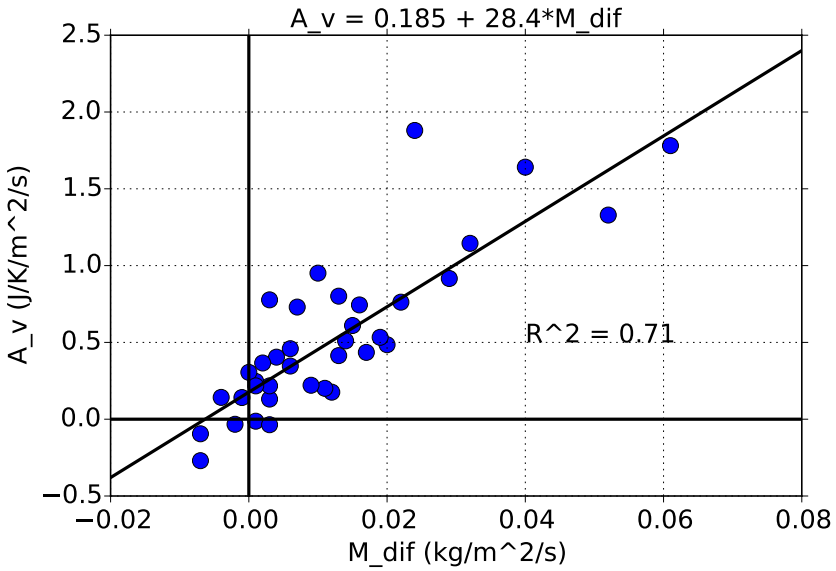

Figure 11: Scatter plot of A_v vs. the difference between the upper and lower level mass fluxes M_{dif}. The regression line is shown and the fraction of variance accounted for is 0.71.

11. This is to be expected, as a positive value of M_{dif} implies mid-level convergence of dry environmental air, which contributes positively to the net entropy divergence.

Figure 12 shows, at least for our data set, that large values of M_{dif} are not favored for SSTs less than about 29°C. Given that the preponderance of our cases occurred over warmer SSTs, this could be a sampling effect. However, if it holds up for a more representative sample, it would have significant implications for the SST dependence of the formation of mesoscale convective regions which tend to exhibit large areas of stratiform precipitation with top-heavy mass flux profiles, i.e., large M_{dif}. Due to the close correlation between M_{dif} and A_v, large A_v tends to be limited to higher SSTs in our sample as well.

Maximum values of A_h are roughly half the maximum values of A_v in our data set, and furthermore A_h does not correlate well with any likely candidate variables such as the precipitation rate or low-level spin up tendency, suggesting that this process had little systematic effect on the development of the systems that we studied.

Finally, we link the entropy and water vapor divergences, and hence the NGMS, to the suspected primary control mechanism for convection, the 500 hPa relative vorticity. Figure 13 shows scatter plots for two samples, cases with the vorticity less or greater than $0.04\,\mathrm{ks}^{-1}$. The cases with stronger mid-level vorticity tend to have smaller entropy divergence (NGMS numerator) for a given value of water vapor divergence (NGMS denominator), indicating smaller NGMS. Smaller NGMS results in a greater precipitation rate for a given value of entropy divergence. In a steady state, the entropy divergence is in balance with the net entropy forcing, defined as the surface minus tropopause entropy fluxes. Thus, a given

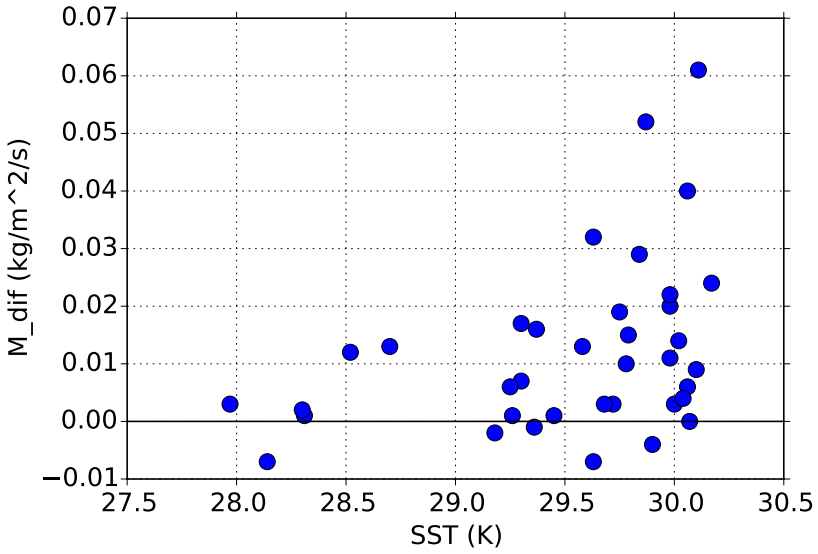

Figure 12: Scatter plot of the upper minus lower level mass flux M_{dif} vs. SST.

forcing results in more intense precipitation and consequently stronger upward mass fluxes at low levels. Furthermore, smaller values of entropy divergence correspond to less top-heavy convection, in agreement with the hypothesis of *Gjorgjievska and Raymond* [2014].

The net import or export of moist entropy from a region is also relevant for diagnosing convective organization. For example, radiative convective equilibrium simulations of tropical convection can exhibit a radiative-convective instability [*Wing and Emanuel*, 2013; *Emanuel et al.*, 2013] in which dry regions embedded within randomly distributed convective systems grow, thus confining convection to a single, intensely convecting region [*e.g., Bretherton et al.*, 2005; *Muller and Held*, 2012; *Wing and Emanuel*, 2013; *Emanuel et al.*, 2013; *Jeevanjee and Romps*, 2013]. *Bretherton et al.* [2005] demonstrated that there is net export of moist static energy out of dry regions in the aggregated state which corresponds to negative gross moist stability. In terms of entropy budgets in dry regions, a negative gross moist stability corresponds to net entropy export that occurs in tandem with moisture export.

Multiple equilibria in precipitation are analogous to dry and precipitating regions in simulations of self-aggregation. Multiple equilibria correspond to steady states that either remain dry in the presence of positive CAPE, or sustain persistent, precipitating deep convection. These occur under identical boundary conditions in limited domain models where the large scale is parameterized using the weak temperature gradient approximation [*Sobel et al.*, 2007; *Sessions et al.*, 2010; *Emanuel et al.*, 2013; *Herman and Raymond*, 2014; *Sessions et al.,* 2015]. In conditions which permit both equilibria, the initial tropospheric moisture determines which equilibrium state is experienced by the model. In the dry state – analogous to the dry region in a larger self-aggregation simulation – moisture is exported from the domain, and moist entropy is either weakly imported or exported, depending on the circula-

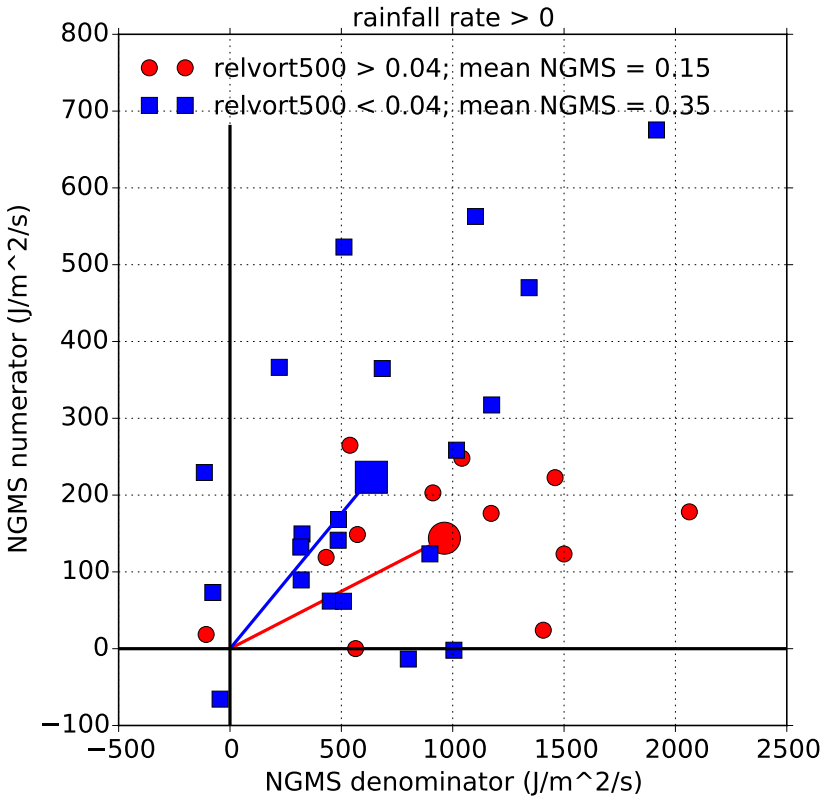

Figure 13: Scatter plot of the NGMS numerator (scaled entropy divergence) to the NGMS denominator (scaled water vapor divergence) for two cases, 500 hPa relative vorticity less than $0.04\,\mathrm{ks}^{-1}$ (blue squares) and greater than this value (red circles). The large blue square and red circle indicate average values of these quantities for the two samples and the slopes of the lines connecting these with the origin are the average values of the NGMS for the two cases. The two samples are limited to cases where the computed rainfall rate is greater than zero to eliminate non-convective situations.

tions in the boundary layer. Net moist entropy import occurs when there is net ascent in the boundary layer; in this case, convergence occurs near the surface where moist entropy is high and lower moist entropy air is exported near the top of the boundary layer, resulting in weak entropy import. Conversely, net descent in the boundary layer exports air with high moist entropy near the surface, and there is net moist entropy divergence. In these conditions, the phenomenon of multiple equilibria is robust and normalized gross moist stability is negative [*Sessions et al.*, 2010]. It is noteworthy that a couple of cases shown in figure 13 exhibit small or negative entropy export in conjunction with net water vapor import, corresponding to small or negative NGMS.

6 Discussion and conclusions

Formulating a correct zeroth order conceptual picture for the large-scale dynamics of the tropical atmosphere has been a long and difficult struggle and has yet to come completely to fruition. However, elements of this picture have begun to fall into place. Given that unbalanced convective dynamics is basically chaotic and unpredictable in detail means that order and predictability must be sought in thermodynamic constraints on convective ensembles and in the balanced dynamics that is hiding within the turbulent swirls and eddies of convection.

Ooyama [1982] led the way in asserting the primacy of balanced dynamics in this quest. His analysis shows the power of the dynamical "cooperative intensification" mechanism of tropical cyclones, but also demonstrates its limitations. The systematic analysis of *Sobel et al.* [2001] using the weak temperature gradient approximation leads inexorably to a balanced system of governing equations, since the fundamental assumption of WTG is that the horizontal divergence is related solely to convective heating.

Various thermodynamic control mechanisms for convection have been investigated. Convective quasi-equilibrium is one of these. Curiously, the full tropospheric quasi-equilibrium of *Arakawa and Schubert* [1974] and *Emanuel et al.* [1994] and the boundary layer quasi-equilibrium of *Emanuel* [1995] and *Raymond* [1995] are converging into a lower tropospheric quasi-equilibrium as espoused by *Kuang* [2008b] and others. This work hints as to how extraordinarily sensitive tropical convection is to the lower tropospheric virtual temperature profile.

Another element of convective behavior that has recently come to light is the sensitivity of convection to tropospheric relative humidity. The model of *Raymond* [2000] was a speculation based on National Weather Service forecasts of summertime precipitation in New Mexico; the higher the dew point, the greater the probability of rain! This seems obvious in retrospect, but the extreme sensitivity of rainfall to saturation fraction demonstrated by *Bretherton et al.* [2004] was unexpected. Evidently it was a surprise to weather and climate modelers as well, as demonstrated by the work of *Derbyshire et al.* [2004]. Increasing the sensitivity of cumulus parameterizations to mid-tropospheric humidity is now well established as essential to improving model forecasts of the Madden-Julian oscillation [*Tokioka et al.*, 1988; *Wang and Schlesinger*, 1999; *Bechtold et al.*, 2008; *Kim et al.*, 2012; *Benedict et al.*, 2014; *Kim et al.*, 2014].

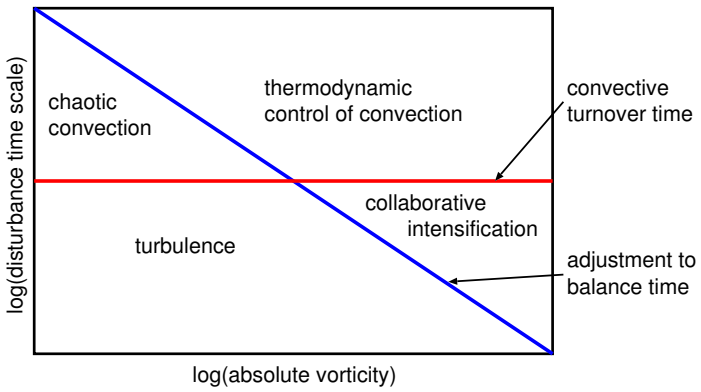

Figure 14: Summary of regimes for tropical disturbances discussed in this paper. The horizontal axis is the characteristic absolute vorticity of the system ζ and the vertical axis is the time scale of the disturbance. The blue line indicates the adjustment to balance time $T_B = 1/\zeta$ while the red line indicates the time scale for convective turnover, typically 1 hr. Disturbances with time scales above the blue line are balanced.

A key element in understanding convection is the observed inverse relationship between environmental moist convective instability and tropospheric humidity. Hints of this result have appeared in the scientific literature over many decades. However, an understanding of the causal relationship underlying this correlation has only begun to develop recently. Moist convective instability is a function of the virtual temperature profile, which in the balanced case depends only on the pattern of potential vorticity and the surface potential temperature distribution. As long as the time scale on which convection modifies the potential vorticity distribution is longer than that for adjustment to balance T_B, it is fair to say that the potential vorticity pattern controls the convection via its effect on the pattern of virtual temperature. An important part of this control acts via the adjustments to the moisture profile caused by the convective response to the pattern of convective instability. This "moisture quasi-equilibrium" process thus becomes an important link in the interaction of convection with dynamics in the tropics. Since higher saturation fraction is associated with stronger precipitation, less instability paradoxically leads to heavier rain.

The gross moist stability [*Raymond et al.*, 2009] has grown into a widely used diagnostic of convective behavior. This quantity is a normalized version of the lateral detrainment of moist entropy (or moist static energy) from a convective region, and therefore tells us how much moist entropy must be supplied to the convective column by surface fluxes and radiation to maintain a certain amount of convection, as measured by upward mass transport or precipitation rate. Our results show that the gross moist stability, though a noisy quantity, is strongly modulated by the mid-level vorticity, most likely due to the effect of this vorticity pattern on the moist convective instability profile and consequently on tropospheric humidity and mass flux profiles.

The result is a complex but comprehensible pattern of interactions between atmospheric dynamics, thermodynamics, and moist convection. Figure 14 shows a regime diagram that summarizes the different forms of convective control (or lack thereof) for disturbances with given time scales and absolute vorticity. "Time scale" in this case means the time required for

convection and other diabatic effects such as radiation and surface fluxes to change significantly the pattern of potential vorticity. Balanced disturbances occur above the blue line and are of two types, those with convection subject to thermodynamic control and those exhibiting dynamic control of convection, i.e., via Ooyama's collaborative intensification mechanism. Below the blue line are turbulence and chaotic convection in which predictability is questionable. The chaotic convection regime includes wave-like disturbances such as equatorial Kelvin waves, which exhibit a certain degree of predictability by mechanisms different than those discussed here. This behavior is worthy of further investigation.

Many of the hypotheses contained herein require further testing via observations and modeling. However, if verified in whole or in part, they point the way to improved conceptual and computational models of the tropical troposphere.

Acknowledgments: We thank Adam Sobel, Brian Mapes, Zhiming Kuang, and an anonymous reviewer for many useful comments. Supporting data and analysis routines are available at http://physics.nmt.edu/∼raymond/data/papers/baldyn_thermo2015.xhtml. This work was supported by National Science Foundation Grants 1342001 and 1056254 and NASA grant NNX12AJ80G.

7 References

Anber, U., S. Wang, and A. Sobel, (2014), Response of atmospheric convection to vertical wind shear: Cloud-system-resolving simulations with parameterized large-scale circulation. Part I: Specified radiative cooling,– *J. Atmos. Sci.,– 71,* 2976-2993.

Arakawa, A., and W. H. Schubert, (1974), Interaction of a cumulus cloud ensemble with the large-scale environment, Part I,– *J. Atmos. Sci.,– 31,* 674-701.

Back, L, E., and C. S. Bretherton, (2006), Geographic variability in the export of moist static energy and vertical motion profiles in the tropical Pacific,– *Geophys. Res. Letters,– 33,* L17810, doi:10.1029/2006GL026672.

Bechtold, P., M. Köhler, T. Jung, F. Doblas-Reyes, M. Leutbecher, M. J. Rodwell, F. Vitart, and G. Balsamo, (2008), Advances in simulating atmospheric variability with the ECMWF model: From synoptic to decadal time-scales,– *Quart. J. Roy. Meteor. Soc.,– 134,* 1337-1351.

Benedict, J. J., E. D. Maloney, A. H. Sobel, and D. M. W. Frierson, (2014), Gross moist stability and MJO simulation skill in three full-physics GCMs,– *J. Atmos. Sci.,– 71,* 3327-3349.

Bister, M., and K. A. Emanuel, (1997), The genesis of hurricane Guillermo: TEXMEX analyses and a modeling study,– *Mon. Wea. Rev.,– 125,* 2662-2682.

Blossey, P. N., C. S. Bretherton, and M. C. Wyant, (2009), Subtropical low cloud response to a warmer climate in a superparameterized cloud model. Part II: Column modeling with a cloud resolving model. *J. Adv. Model. Earth Syst., 1, Art. #8.*

Bolin, B., (1955), Numerical forecasting with the barotropic model,– *Tellus,– 7,* 27-49.

Bolin, B., (1956), An improved barotropic model and some aspects of using the balance equations for three-dimensional flow,– *Tellus,– 8,* 61-75.

Bretherton, C. S., P. N. Blossey, and M. Khairoutdinov, (2005), An energy-balance analysis of deep convective self-aggregation above uniform SST,- *J. Atmos. Sci.,– 62,* 4273-4292.

Bretherton, C. S., M. E. Peters, and L. E. Back, (2004), Relationships between water vapor path and precipitation over the tropical oceans,– *J. Climate,– 17,* 1517-1528.

Bretherton, C. S., and P. K. Smolarkiewicz, (1989), Gravity waves, compensating subsidence and detrainment around cumulus clouds,– *J. Atmos. Sci.,– 46,* 740-759.

Brown, R. G., and C. S. Bretherton, (1997), A test of the strict quasi-equilibrium theory on long time and space scales,– *J. Atmos. Sci.,– 54,* 624-638.

Burpee, R. W., (1972), The origin and structure of easterly waves in the lower troposphere of North Africa,– *J. Atmos. Sci.,– 29,* 77-90.

Burpee, R. W., (1974), Characteristics of the North African easterly waves during the summers of 1968 and 1969,– *J. Atmos. Sci.,– 31,* 1556-1570.

Burpee, R. W., (1975), Some features of synoptic-scale waves based on compositing analysis of GATE data,– *Mon. Wea. Rev.,– 103,* 921-925.

Charney, J. G., (1955), The use of primitive equations of motion in numerical prediction,– *Tellus,– 7,* 22-26.

Charney, J. G., (1962), Integration of the primitive and balance equations, *Proc. Symp. on Num. Weather Prediction*, Tokyo, 131-150.

Charney, J. G., (1963), A note on large-scale motions in the tropics, *J. Atmos. Sci., 20,* 607-609.

Charney, J. G. and A. Eliassen, (1964), On the growth of the hurricane depression,– *J. Atmos. Sci.,– 21,* 68-75.

Chang, S. W., and H. D. Orville, (1973), Large-scale convergence in a numerical model, *J. Atmos. Sci., 5,* 947-950.

Cheng, M.-D., and A. Arakawa, (1997), Inclusion of rainwater budget and convective downdrafts in the Arakawa-Schubert cumulus parameterization,– *J. Atmos. Sci.,– 54,* 1359-1378.

Cho, H.-R., and M. A. Jenkins, (1987), The thermal structure of tropical easterly waves,– *J. Atmos. Sci.,– 44,* 2531-2539.

Davis, C. A., (1992), Piecewise potential vorticity inversion,- *J. Atmos. Sci.,– 49,* 1397-1411.

Derbyshire, S. H., I. Beau, P. Bechtold, J.-Y. Grandpeix, J.-M. Piriou, J.-L. Redelsperger, and P. M. M. Soares, (2004), Sensitivity of moist convection to environmental humidity, *Quart. J. Roy. Meteor. Soc.,– 130,* 3055-3079.

Edman, J. P., and D. M. Romps, (2014), An improved weak pressure gradient scheme for single-column modeling,– *J. Atmos. Sci.,– 71,* 2415-2429.

Emanuel, K. A., (1986), An air-sea interaction theory for tropical cyclones. Part I: Steady state maintenance,– *J. Atmos. Sci.,– 43,* 585-604.

Emanuel, K. A., (1995), The behavior of a simple hurricane model using a convective scheme based on subcloud-layer entropy equilibrium,– *J. Atmos. Sci.,– 52,* 3960-3968.

Emanuel, K., A. A. Wing, and E. M. Vincent, (2013), Radiative-convective instability,– *J. Adv. Model. Earth Syst.,– 5,* doi:10.1002/2013MS000270.

Emanuel, K. A., J. D. Neelin, and C. S. Bretherton, (1994), On large-scale circulations in convecting atmospheres,– *Quart. J. Roy. Meteor. Soc.,– 120,* 1111-1143.

Gent, P. R., and J. C. McWilliams, (1983a), Consistent balanced models in bounded and periodic domains,– *Dyn. Atmos. Oceans,– 7,* 67-93.

Gent, P. R., and J. C. McWilliams, (1983b), Regimes of validity for balanced models,– *Dyn. Atmos. Oceans,– 7,* 167-183.

Gent, P. R., and J. C. McWilliams, (1983c), The equatorial waves of balanced models,– *J. Phys. Ocean.,– 13,* 1179-1191.

Gjorgjievska, S., and D. J. Raymond, (2014), Interaction between dynamics and thermodynamics during tropical cyclogenesis,– *Atmos. Chem. Phys.,– 14,* 3065-3082.

Haynes, P. H., and M. E. McIntyre, (1987), On the evolution of vorticity and potential vorticity in the presence of diabatic heating and frictional or other forces,– *J. Atmos. Sci.,– 44,* 828-841.

Haynes, P. H., and M. E. McIntyre, (1990), On the conservation and impermeability theorems for potential vorticity,– *J. Atmos. Sci.,– 47,* 2021-2031.

Held, I. A., and B. J. Hoskins, (1985), Large-scale eddies and the general circulation of the troposphere, *Advances in Geophysics, 28a*, 3-31.

Herman, M. J., and D. J. Raymond, (2014), WTG Cloud modeling with spectral decomposition of heating, *J. Adv. Modeling Earth Systems*, doi:10.1002/2014MS000359.

Holton, J. R., and R. S. Lindzen, (1972), An updated theory for the quasi-biennial cycle of the tropical stratosphere. 29, 1076-1080.

Hoskins, B. J., M. E. McIntyre, and A. W. Robertson, (1985), On the use and significance of isentropic potential vorticity maps,– *Quart. J. Roy. Meteor. Soc.,– 111,* 877-946.

Jeevanjee, N., and K. M. Romps, (2013), Convective self-aggregation, cold pools, and domain size,– *Geophys. Res. Letters,– 40,* 1-5, doi:10.1002/grl.50204.

Jenkins, M. A., and H.-R. Cho, (1991), An observational study of the first-order vorticity dynamics in a tropical easterly wave,– *J. Atmos. Sci.,– 48,* 965-975.

Khouider, B., and A. J. Majda, (2008), Equatorial convectively coupled waves in a simple multicloud model, *J. Atmos. Sci., 65,* 3376-3397.

Kim, D., A. H. Sobel, A. D. Del Genio, Y. Chen, S. J. Camargo, M.-S. Yao, M. Kelley, and L. Nazarenko, (2012), The tropical subseasonal variability simulated in the NASA GISS general circulation model, *J. Climate, 25,* 4641-4659.

Kim, D., and Co-Authors, (2014), Process-oriented MJO simulation diagnostic: Moisture sensitivity of simulated convection,– *J. Climate,– 27,* 5379-5395.

Kuang, Z., (2008a), Modeling the interaction between cumulus convection and linear gravity waves using a limited-domain cloud system-resolving model,– *J. Atmos. Sci.,– 65,* 576-591.

Kuang, Z., (2008b), A moisture-stratiform instability for convectively coupled waves,– *J. Atmos. Sci.,– 65,* 834-854.

Kuang, Z., (2011), The wavelength dependence of the gross moist stability and the scale selection in the instability of column-integrated moist static energy, *J. Atmos. Sci., 68,* 61-74.

LeMone, M. A. and E. J. Zipser, (1980), Cumulonimbus vertical velocity events in GATE. Part I: Diameter, intensity and mass flux,– *J. Atmos. Sci.,– 37,* 2444-2457.

Lin, J.-L., T. Qian, T. Shinoda, and S. Li, (2015), Is the tropical atmosphere in convective quasi-equilibrium? *J. Climate, 28,* 4357-4372.

Lindzen, R. S., and J. R. Holton, (1968), A theory of the quasi-biennial oscillation,– *J. Atmos. Sci.,– 25,* 1095-1107.

Lorenz, E. N., (1960), Energy and numerical weather prediction,– *Tellus,– 12,* 364-373.

Mapes, B. E., (2000), Convective inhibition, subgrid-scale triggering energy, and stratiform instability in a toy tropical wave model,– *J. Atmos. Sci.,– 57,* 1515-1535.

Matsuno, T., (1966), Quasi-geostrophic motions in the equatorial area, *J. Meteor. Soc. Japan, 44,* 25-43.

McIntyre, M. E., and W. A. Norton, (2000), Potential vorticity inversion on a hemisphere, *J. Atmos. Sci.,– 57,* 1214-1235.

McWilliams, J. C., (1985), A uniformly valid model spanning the regimes of geostrophic and isotropic, stratified turbulence: Balanced turbulence,– *J. Atmos. Sci.,– 42,* 1773-1774.

McWilliams, J. C. and P. R. Gent, (1980), Intermediate models of planetary circulations in the atmosphere and ocean,– *J. Atmos. Sci.,– 37,* 1657-1678.

Molinari, J., D. Knight, M. Dickinson, D. Vollaro, and S. Skubis, (1997), Potential vorticity, easterly waves, and eastern Pacific tropical cyclogenesis,– *Mon. Wea. Rev.,– 125,* 2699-2708.

Montgomery, M. T., C. Davis, T. Dunkerton, Z. Wang, C. Velden, R. Torn, S. J. Majumdar, F. Zhang, R. K. Smith, L. Bosart, M. M. Bell, J. S. Haase, A. Heymsfield, J. Jensen, T. Campos, and M. A. Boothe, (2012), The pre-depression investigation of cloud systems in the tropics (PREDICT) experiment,– *Bull. Am. Meteor. Soc.,– 93,* 153-172.

Montgomery, M. T., and R. K. Smith, (2014), Paradigms for tropical cyclone intensification, *Australian Meteorological and Oceanographic Journal*, *64*, 37-66.

Moorthi, S., and M. J. Suarez, (1992), Relaxed Arakawa-Schubert. A parameterization of moist convection for general circulation models,– *Mon. Wea. Rev.,– 120,* 978-1002.

Muller, C. J., and I. M. Held, (2012), Detailed investigation of the self-aggregation of convection in cloud-resolving simulations,– *J. Atmos. Sci.,– 69,* 2551-2565.

Neelin, J. D., and N. Zeng, (2000), A quasi-equilibrium tropical circulation model – formulation,– *J. Atmos. Sci.,– 57,* 1741-1766.

Norquist, D. C., E. E. Recker, and R. J. Reed, (1977), The energetics of African wave disturbances as observed during Phase III of GATE,– *Mon. Wea. Rev.,– 105,* 334-342.

Ooyama, K., (1964), A dynamical model for the study of tropical cyclone development, *Geofisica Internacional*, *4*, 187-198.

Ooyama, K., (1969), Numerical simulation of the life cycle of tropical cyclones,– *J. Atmos. Sci.,– 26,* 3-40.

Ooyama, K., (1982), Conceptual evolution of the theory and modeling of the tropical cyclone,– *J. Meteor. Soc. Japan,– 60,* 369-379.

Peixoto, J. P., and A. H. Oort, (1992), *Physics of climate*, American Institute of Physics, 520 pp.

Ramage, C. S., (1971), *Monsoon meteorology*, Academic Press, New York, 296 pp.

Randall, D. A., K.-M. Xu, R. J. C. Somerville, and S. Iacobellis, (1996), Single-column models and cloud ensemble models as links between observations and climate models, *J. Climate,– 9,* 1683-1697.

Raymond, D. J., (1992), Nonlinear balance and potential-vorticity thinking at large Rossby number,– *Quart. J. Roy. Meteor. Soc.,– 118,* 987-1015.

Raymond, D. J., (1994), Nonlinear balance on an equatorial beta plane,– *Quart. J. Roy. Meteor. Soc.,– 120,* 215-219.

Raymond, D. J., (1995), Regulation of moist convection over the west Pacific warm pool,– *J. Atmos. Sci.,– 52,* 3945-3959.

Raymond, D. J., (2000), Thermodynamic control of tropical rainfall,– *Quart. J. Roy. Meteor. Soc.,– 126,* 889-898.

Raymond, D. J., G. B. Raga, C. S. Bretherton, J. Molinari, C. López-Carrillo, and Ž. Fuchs, (2003), Convective forcing in the intertropical convergence zone of the eastern Pacific, *J. Atmos. Sci.,– 60,* 2064-2082.

Raymond, D. J., C. S. Bretherton, and J. Molinari, (2006), Dynamics of the intertropical convergence zone of the east Pacific,– *J. Atmos. Sci.,– 63,* 582-597.

Raymond, D. J., (2012), Balanced thermal structure of an intensifying tropical cyclone,– *Tellus,– 64,* 19181, doi.org/10.3402/tellusa.v64i0.19181.

Raymond, D. J., (2013), Sources and sinks of entropy in the atmosphere,– *J. Adv. Model. Earth Syst.,–* doi:10.1002/jame.20050.

Raymond, D. J., and M. J. Herman, (2011), Convective quasi-equilibrium reconsidered,– *J. Adv. Model. Earth Syst.,– 3,* Art. 2011MS000079, 14 pp.

Raymond, D. J., C. López-Carrillo, and L. López Cavazos, (1998), Case-studies of developing east Pacific easterly waves,– *Quart. J. Roy. Meteor. Soc.,– 124,* 2005-2034.

Raymond, D. J. and S. L. Sessions, (2007), Evolution of convection during tropical cyclogenesis,– *Geophys. Res. Letters,– 34,* L06811, doi:10.1029/2006GL028607.

Raymond, D. J., S. Gjorgjievska, S. Sessions, and Ž. Fuchs, (2014), Tropical cyclogenesis and mid-level vorticity, *Australian Meteorological and Oceanographic Journal*, *64*, 11-25.

Raymond, D. J., S. L. Sessions, and Ž. Fuchs, (2007), A theory for the spinup of tropical depressions,– *Quart. J. Roy. Meteor. Soc.,– 133,* 1743-1754.

Raymond, D. J., S. L. Sessions, and C. López Carrillo, (2011), Thermodynamics of tropical cyclogenesis in the northwest Pacific,– *J. Geophys. Res.,– 116,* D18101, doi:10.1029/2011JD015624.

Raymond, D. J., S. Sessions, A. Sobel, and Ž. Fuchs, (2009), The mechanics of gross moist stability, *J. Adv. Model. Earth Syst.*, *1*, art. #9, 20 pp.

Raymond, D. J., and X. Zeng, (2005), Modelling tropical atmospheric convection in the context of the weak temperature gradient approximation,– *Quart. J. Roy. Meteor. Soc.,– 131,* 1301-1320.

Reed, R. J., D. C. Norquist, and E. E. Recker, (1977), The structure and properties of African wave disturbances as observed during Phase III of GATE,– *Mon. Wea. Rev.,– 105,* 317-333.

Romps, D. M., (2012a), Weak pressure gradient approximation and its analytical solution, *J. Atmos. Sci.,– 69,* 2835-2845.

Romps, D. M., (2012b), Numerical tests of the weak pressure gradient approximation,– *J. Atmos. Sci.,– 69,* 2846-2856.

Rotunno, R., and K. A. Emanuel, (1987), An air-sea interaction theory for tropical cyclones. Part II: Evolutionary study using a nonhydrostatic axisymmetric numerical model,– *J. Atmos. Sci.,– 44,* 542-561.

Sessions, S. L., S. Sugaya, D. J. Raymond, and A. H. Sobel, (2010), Multiple equilibria in a cloud-resolving model using the weak temperature gradient approximation,– *J. Geophys. Res., 115,* D12110, doi:10.1029/2009JD013376.

Sessions, S. L., M. J. Herman, and S. Sentic, (2015), Convective response to changes in the thermodynamic environment in idealized weak temperature gradient simulations, *J. Adv. Model. Earth Syst., 07*, doi:10.1002/2015MS000446.

Singh, M. S., and P. A. O'Gorman, (2013), Influence of entrainment on the thermal stratification in simulations of radiative-convective equilibrium,– *Geophys. Res. Letters,– 40,* 4398-4403.

Smith, R. K., and M. T. Montgomery, (2008), Balanced boundary layers used in hurricane models,– *Quart. J. Roy. Meteor. Soc.,– 134,* 1385-1395.

Sobel, A. H., G. Bellon, and J. Bacmeister, (2007), Multiple equilibria in a single-column model of the tropical atmosphere,– *Geophys. Res. Letters,– 34,* L22804, doi:10.1029/2007GL031320.

Sobel, A. H., and C. S. Bretherton, (2000), Modeling tropical precipitation in a single column,– *J. Climate,– 13,* 4378-4392.

Sobel, A. H., J. Nilsson, and L. M. Polvani, (2001), The weak temperature gradient approximation and balanced tropical moisture waves,– *J. Atmos. Sci.,– 58,* 3650-3665.

Sobel, A. H., S. E. Yuter, C. S. Bretherton, and G. N. Kiladis, (2004), Large-scale meteorology and deep convection during TRMM KWAJEX, *Mon. Wea. Rev., 132,* 422-444.

Soong, S.-T., and Y. Ogura, (1980), Response of Tradewind cumuli to large-scale processes, *J. Atmos. Sci., 37,* 2035-2050.

Thayer-Calder, K., and D. Randall, (2015), A numerical investigation of boundary layer quasi-equilibrium, *Geophys. Res. Letters*, doi:10.1002/2014GL062649.

Thompson, R. M., S. W. Payne, E. E. Recker and R. J. Reed, (1979), Structure and properties of synoptic-scale wave disturbances in the intertropical convergence zone of the eastern Atlantic,– *J. Atmos. Sci.,– 36,* 53-72.

Thorncroft, C. D., and B. J. Hoskins, (1994a), An idealized study of African easterly waves. I: A linear view,– *Quart. J. Roy. Meteor. Soc.,– 120,* 953-982.

Thorncroft, C. D., and B. J. Hoskins, (1994b), An idealized study of African easterly waves. II: A nonlinear view,– *Quart. J. Roy. Meteor. Soc.,– 120,* 983-1015.

Tokioka, T., K. Yamazaki, A. Kitoh, and T. Ose, (1988), The equatorial 30-60 day oscillation and the Arakawa-Schubert penetrative cumulus parameterization,– *J. Meteor. Soc. Japan,– 66,* 883-901.

Wang, W., and M. E. Schlesinger, (1999), The dependence on convection parameterization of the tropical intraseasonal oscillation simulated by the UIUC 11-layer atmospheric GCM, *J. Climate, 12,* 1423-1457.

Wang, S., A. H. Sobel, and Z. Kuang, (2013), Cloud-resolving simulation of TOGA-COARE using parameterized large-scale dynamics, *J. Geophys. Res.*, *118*, 6290-6301, doi:10.1002/jgrd.50510.

Wheeler, M., and G. N. Kiladis, (1999), Convectively coupled equatorial waves: Analysis of clouds and temperature in the wavenumber-frequency domain,– *J. Atmos. Sci.,– 56,* 374-399.

Williams, E. R., S. A. Rutledge, S. G. Geotis, N. Renno, E. Rasmussen, and T. Rickenbach, (1992), A radar and electrical study of tropical "hot towers",- *J. Atmos. Sci.,– 49,* 1386-1395.

Wing, A. A., and K. A. Emanuel, (2013), Physical mechanisms controlling self-aggregation of convection in idealized numerical modeling simulations,– *J. Adv. Model. Earth Syst.,– 5,* 1-14, doi 10.1002/2013MS000269.

Xu, K.-M., and K. A. Emanuel, (1989), Is the tropical atmosphere conditionally unstable?, *Mon. Wea. Rev.,– 117,* 1471-1479.

Yasunaga, K., and B. E. Mapes, (2012a), Differences between more-divergent vs. more-rotational types of convectively coupled equatorial waves. Part I: Space-time spectral analyses,– *J. Atmos. Sci.,– 69*, 3-16.

Yasunaga, K., and B. E. Mapes, (2012b), Differences between more-divergent vs. more-rotational types of convectively coupled equatorial waves. Part II: composite analysis based on space-time filtering,– *J. Atmos. Sci.,– 69,* 17-34.

Zeng, N., J. D. Neelin, and C. Chou, (2000), A quasi-equilibrium tropical circulation model – implementation and simulation,– *J. Atmos. Sci.,– 57,* 1767-1796.

Zipser, E. J. and M. A. LeMone, (1980), Cumulonimbus vertical velocity events in GATE. Part II: Synthesis and model core structure,– *J. Atmos. Sci.,– 37,* 2458-2469.